Doctoral Dissertation

Ohmic Contact Formation of Gallium Nitride and Electrical Properties Improvement

Aiman bin Mohd Halil

December 2015

Graduate School of Engineering

Osaka University

Ohmic Contact Formation of Gallium Nitride and

Electrical Properties Improvement

Contents:

Chapter 1: Introduction

1.1 Background

In the 68 years since then invention of the transistor by John Bardeen, William Shockley and Walter Brattain in 1947, much attention has been given to silicon (Si) devices and integrated circuits (ICs). The impact of silicon electronic triggered the era of information processing and continues to produce amazing progress. The size of the circuit elements, the speed of their operation, the minimal power consumed, the cost per element, and the reliability of the circuits have improved dramatically. In the 1990s, silicon integrated circuits, about the size of fingernail, contain a million transistors and cost a few dollars or tens of dollars depending on the type of production level. In the late 90s, researchers believe that there are good reasons to expect that some chips will contain a billion elements by the end of that decade. Today in 2015, the improvement in integrated circuits technology had gone beyond expectations for everyone. For the last 20 years, computer chips become more powerful yet cheaper than the year before. Gordon Moore, one of the early integrated circuit pioneers and founders of Intel once said, "If the auto industry advanced as rapidly as the semiconductor industry, today a Roll-Royce would get a half a million miles per gallon, and it would be cheaper to throw it away than to park it".

And yet, still the basis of all this improvement is retained. Integrated circuit chips are not useful until they have been woven into the fabric of interconnections and packaged. Packaging and interconnection provide structural support, mechanical and chemical protection, thermal management, power, ground and signal transmission, including timing. The package must be durable and manufacturable and allow access for testing and

repair. From the year researchers started to build circuit using semiconductor until today, there have been invented so many packaging techniques. One of the oldest techniques are sheet metal technique, cast metal technique and machines metal technique. Today, printed circuit is primarily the technique that is used for connecting components together. This technique also provides mechanical structure.

Semiconductor devices

In semiconductor industry, packaging technique has been the main subject to be improved for a long time. Today, researchers agree that not only technique, but also the elements that are used in have to be improved. Since 1947, silicon has been commonly used as the main element for creating electronic circuit. There are some reasons why silicon is commonly used. First, silicon is very easy to find in nature. Ordinary sand, like on the beach or in the desert for example, are nothing more than one silicon atom combines with two oxygen atoms. However, if we want silicon in its pure form suitable for the production of computer chips, it has to be purified in a carefully monitored process. The other reason for the popularity of silicon is that it is stable and can be heated to a rather degree without losing its material characteristics. This means that engineers can be sure it will perform the planned function, even under severe conditions.

As we can see, the evolution of the semiconductor from the day transistor was invented until today, semiconductor components, like chips and transistors become smaller and smaller. This evolution contribute to a world where computers become faster and smaller each year. But this also means that we eventually reach a limit on how much faster, smaller and effective the silicon based electronic circuits can be made.

Another field that also gets impact with the development of semiconductor

technology is the power electronic device and communication network. Power devices are semiconductor devices used as switches or rectifiers in power electronic circuits. Power devices convert electric power from one form to another form and play a critical role in conserving energy and environment. Advances in this power devices technology have led to the rapid multiplication of power electronic devices into computers, transportations, utilities, industrial applications and all forms of environment-friendly energy conversion.

In the sector of communication network, improvement in the frequency and power-handling capabilities of transistor have led to the advancement of the amplifiers, modulators, and other key components of the advanced communications networks. Progresses in this sector promise a better high-performance base stations of future wireless networks with a high-speed streams of data, high-reliability and efficient power consumptions.

In the efforts to reduce the effect of global warming and other global energy problem, the development of power devices technology and communication sector seem to be some of the crucial subjects to be considered. In near future, power electronic and communication systems must be more energy efficient to balance the environment conservation with ever-increasing demand of energy world.

Wide-band Gap Semiconductors

Today, most of power electronic devices are still made of silicon. However, due to limitations of the physical properties of silicon, it is important to replace the devices with those made of better alternative materials for use in the future power electronic and communication devices. Two semiconductor materials of the most promising candidates

for that purpose are gallium nitride (GaN) and silicon carbide (SiC).

Both GaN and SiC are going to be used in the next generation power electronic and communication devices due to their wide band-gap, thus allowing operation at higher temperatures, power densities, frequencies and voltages with lower leak currents than silicon-based devices [1]. The band gap of a semiconductor pertains to the required energy for an electron to jump from the top of the valence band to the bottom of the conduction band within the material. Materials of which band gap is typically wider than two electron-volts (eV) are referred as wide band gap material. GaN and SiC semiconductors are also commonly referred as compound semiconductors because they are composed of multiple elements from the periodic table.

Wide band gap devices promise substantial performance improvement over their silicon based electronic devices. Table 1.1 shows the comparison between silicon, SiC and GaN properties. The higher critical field on both GaN and SiC compared to silicon is a property which allows these devices to operate at higher voltages and lower leakage currents. Higher electron mobility and electron saturation velocity allow higher frequency of operation. While silicon has higher electron mobility than SiC, GaN's electron mobility is higher than silicon meaning that GaN is the best semiconductor for very high frequency devices. Higher thermal conductivity means that the material is superior in conducting heat more efficiently. SiC has higher thermal conductivity than GaN meaning that SiC devices can theoretically operate at higher power densities than either silicon or GaN. Higher thermal conductivity combined with wide band gap and high critical field give SiC semiconductor an advantage when used in devices with high power operations.

The advantages of GaN properties make GaN one of the best materials to be use in the communication sector. Today, silicon-based amplifiers in the cellular base-station

are already being pushed to their limits. The silicon technology used today reached it limit at 10 percent energy efficiency, meaning that 90 percent of the power that goes into the system is wasted as heat. Additionally, big and powerful fans must be use continuously to remove the heat from the amplifier, which further introduce more distortions to the system. GaN-based transistors could double or triple the efficiency of base-station amplifiers, so that a given area could be covered by fewer base stations, with more data at much higher rates. Furthermore, without the necessity of using big and powerful cooling fans, it is even possible to shrink the entire base station thus further reduced the cost of the system.

Table 1.1 Some important properties of silicon, SiC and GaN [2-5].

Properties	**Silicon**	**SiC (SiC-4H)**	**GaN**
Band gap (eV)	1.1	3.2	3.4
Critical field (10^8 V/m)	0.3	3	3.5
Electron mobility at 300 K (10^{-4} cm^2/Vs)	1450	900	2000
Electron saturation Velocity (10^4 m/s)	10	22	25
Thermal conductivity (10^4 W/m^2K)	1.5	5	1.3

However, GaN and SiC have to be connected to metallic materials to form electronic circuits. The ideal contact between these semiconductors and metals is one that allows smooth transportation across the interface. Such an interface shows a constant resistance indicated by proportional current-voltage (*I*–*V*) characteristics obeying the Ohm's law. Contact interfaces between semiconductors and metals with such properties are referred to as ohmic contacts. For p-type semiconductors, an ohmic contact can be

formed by connecting with a metallic material of which work function ($\varnothing_m$) is the same or higher than the electron affinity (χ) and the bandgap (E_g) of the semiconductor, *i.e.*,

$$e\phi_m \geq \chi + E_g \tag{1.1}$$

where *e* is the elementary charge. However, the energy levels of the valence band edges ($\chi + E_g$) for p-type GaN and SiC are very deep: 7.50 and 6.46 eV, respectively. There is no pure metal which satisfies condition of Eq. (1.1). In the case that the work function of the connected metal is lower than the total of the electron affinity and the bandgap of the semiconductor, the electrons in the metal flow into the semiconductor until the Fermi levels of these two materials become equal, forming a depleted zone of carriers (holes) in the semiconductor under the contact. The zone interferes with carrier transportation across the interface. This interference is known as Schottky barrier (SB). Carriers moving across such a contact interface require energy to get over the barrier. Thus, Joule heat is generated at the interface, which deteriorates the energy efficiency and the reliability of the device. Therefore, a technology is demanded to establish low-resistance ohmic contacts by lowering the SB height and/or by thinning the carrier depleted zone.

In the case of n-type semiconductors, an ohmic contact can be formed by connecting with a metallic material which work function is the same or lower than the electron affinity of the semiconductors, *i.e.*,

$$e\phi_m \leq \chi \tag{1.2}$$

where *e* is the elementary charge. Contrary with ohmic contact formation of p-type semiconductors, the ohmic contact formation of n-type semiconductors can be achieve

easier due to a lot of materials that can satisfies condition of Eq. (1.2). However, to increase the energy efficiency of the devices, a technology is demanded to lower the contact resistance of n-type contact.

The problems related to formation of low-resistance ohmic contact between metal and GaN or SiC interfaces has been researched actively worldwide and some important solutions have been reported. It was found that Ti_3SiC_2 formed adjacent to SiC provides a good ohmic contact for p-type SiC [6-11]. Furthermore, Ti-based contact materials were reported to produce a good ohmic contact for n-type SiC [12]. With the discovery of adequate contact materials for p-type and n-type SiC, the realization of SiC-based electronic devices might can be achieved in the near future. The same thing cannot be said to GaN-based devices. Despite some promising results reported for ohmic contact formation on n-type GaN, there are no adequate contact materials for ohmic formation on p-type GaN found so far. Without an adequate contact materials for p-type GaN discovered, the application of GaN-based semiconductor devices is still far from real.

1.2 Present Issues

p-type GaN

The problems related to formation of ohmic contact between metal and p-type GaN semiconductor has been researched actively worldwide and some important solutions have been reported. It was found that Ti_3SiC_2 formed adjacent to SiC provides a good ohmic contact for p-type SiC [6-11]. Ti_3SiC_2 is considered to work as a narrow-bandgap intermediate semiconductor layer which reduces the SB height [7, 8]. On the other hand, no appropriate material for low-resistance ohmic contacts to p-type GaN has been found so far. Jang *et al.* reported that low-resistance and thermally stable ohmic characteristic is achieved with a Au/Ni/Ru/Ag/Ni multilayered contact on p-type GaN [13]. In another paper, Chen *et al.* suggested that a low-resistance ohmic contact is achieved with the formation of NiO and a specific microstructure by annealing Au/Ni/p-type GaN in an oxidative ambient [14]. However, most of the solutions are usually difficult to be reproduced by other researchers, even if the reported procedures are followed. This implies that the reported processes do not correspond only to the formation of the preferred structure at the contact interface. Therefore, a technology to control the interfacial structure has to be established based on knowledge of the formation mechanism of low-resistance ohmic interfaces between metals and p-type GaN. However, since the suggested contacts are formed by complex interfacial reaction between the substrate and multilayered films, establishing a firm basic of this technology seem to be a difficult task to tackle [13].

The other important problem in realizing GaN-based power electronic devices are related to the low electrical conductivity of p-GaN. The only effective p-type dopant

known for p-GaN is magnesium (Mg). Although some decent annealing methods were developed [15-16] after the breakthrough discovery of Mg activation by electron beam irradiation [17], new developments of improvement methods for p-type GaN conductivity have not been accomplished. It is reported that only approximately one percent of doped magnesium atoms are activated during Mg activation [18, 19]. This is due to the presence of hydrogen (H) within the Mg-doped p-GaN, incorporated during growth [20]. H is known to electrically passivate the acceptors [21]. This passivation is attributed to the formations of neutral Mg-H complexes where H is bonded interstitially to a neighboring nitrogen atom [22-24]. Furthermore, in order to achieve p-type conductivity, postgrowth activation of Mg by thermal annealing, which releases H from GaN, is necessary [15]. The thermal annealing is believed to releases H from GaN but not so effective.

Moreover, numerous investigations of p-type GaN have suggested that the elevated temperature during the contact formation process can cause development of N-vacancies within GaN sub-surface, which consequently reduce the hole concentration of the p-type GaN [25]. These vacancies are known to act as n-type dopant atoms with a donor level very close to the conduction band edge of n-type GaN [26]. Fujimoto et al. reported that Hall-effect measurements revealed that an n-type conductive layer was formed near the p-GaN surfaces by annealing at 1073 K in vacuum [27]. Therefore, it is important to understand and improve the processes of H release from p-GaN and contact formation under lower temperature conditions.

n-type GaN

On the other hand, to lower the contact resistance of n-type GaN contact, it is effective to increase the carrier density in the GaN just under the contact material. The density can be increased by implantation of dopants. Formation of TiN by interfacial reaction between GaN and Ti generates N-vacancies in GaN, which work as donors at an energy level close to the conduction band edge of GaN [28]. Therefore, TiN is formed adjacent to GaN by interfacial reaction between GaN and multilayered metallic film containing Ti layer [29-32]. Furthermore, Maeda et al. have reported that N-vacancies formed in the sub-interface of GaN by interfacial reaction between GaN and contact metal, instead of the formation of TiN adjacent to GaN, play an essential role in developing ohmic properties [33]. Generally, the vacancies are formed by interfacial reactions between the deposited film and the GaN substrate during the contact formation process. However, the interfacial reaction is not the only method to form N-vacancies and lower the contact resistance. Other methods still not be fully developed, thus the most effective method is still unidentified. Therefore, the development of other methods to form N-vacancies is needed to establish a clear understanding of most effective methods to lower the contact resistance of n-type GaN contact.

The other promising aspect to consider to form low-resistance ohmic contact of n-type GaN is the face orientation of GaN contact. The (0001) Ga-face of GaN has been used in most of the papers reporting ohmic contact formation. This is due to the restriction in the growth of GaN single-crystals, which are generally epitaxially grown on sapphire substrates by metal-organic chemical vapor deposition. Recently, some techniques to produce free-standing bulk GaN single-crystals have been developed. Although they are still not the mainstream of mass production, the quality and size of the single-crystals will

be rapidly improved. Thus, GaN single-crystals with other surface orientations will soon be available. On the other hand, it has not been clarified whether or not the (0001) plane is the best orientation for achieving low-resistance conduction in the sheet and at the contact interface. Thus, a broad observations of electrical properties of n-type GaN contact with various contacts orientations are needed to clarify the most suitable contact orientation of n-type GaN.

1.3 Objective of Present Study

In the present study, the strategy to improve the electrical properties of n-type and p-type GaN contacts has been carried out.

In the case of n-type GaN contact, to seek for the most effective methods to improve the electrical properties of the contact, an alternative method to form N-vacancies near the interface to lower the contact resistance have been developed. Additionally, to clarify the most suitable surface orientation of n-type GaN contact, unconventional contact orientation have been observed and compared.

In the case of p-type GaN contact, a different approach to finding an appropriate contact material for p-type GaN has been used in the present study. GaN shows a higher degree of similarity with SiC than with Gallium Arsenide (GaAs) in both crystallographic and electronic structures, as shown in Table 1.2 [2-5]. These are the most crucial factors which directly affect the formed contact structure and electrical properties. Thus, there is a high possibility that SiC contact materials are more suitable than GaAs contact materials for the formation of an ohmic contact to GaN. The present study demonstrates this idea by forming Ti_3SiC_2 contacts on p-type GaN and examining the properties of the contacts. It has been reported that good ohmic contact has been achieved with p-type SiC and

Ti_3SiC_2 contacts by annealing at 1273 K [6-10]. Although there is possibility that the hole concentration of the p-type GaN is reduced by annealing at these temperatures, the investigation of the contact properties and interfacial structure of GaN and Ti3SiC2 are an important step to understand the practicality of this contact structure. For comparison, the contact properties of conventional monolayer contact of p-type GaN such as Au, Ni and also have been observed.

Table 1.2 Properties of GaN and SiC [2-5].

Properties	**GaN**	**4H-SiC**	**GaAs**
Crystal system	Hexagonal	Hexagonal	Cubic
Lattice parameter, *a* nm	0.3189	0.3073	0.5653
Lattice parameter, *c*/nm	0.5186	1.0053	-
Coefficient of thermal expansion, α/K^{-1}	5.59×10^{-6}	4.47×10^{-6}	6.50×10^{-6}
Bandgap, E_g/eV	3.39	3.26	1.42
Electron affinity, χ/eV	4.11	3.20	4.07

Additionally, in the present study, in order to improve the electrical properties of p-GaN contact, the enhancement of H release from p-GaN is attempted by applying current flow through the p-GaN substrates during low temperatures annealing. By enhancing the H release from p-GaN, the electrical properties of p-GaN contact interface can be improved. The higher carrier (accepter) concentration achieved by enhancing the H release from p-GaN will reduce the width of the SB formed at the contact interface. By thinning the SB width, the probability of carrier to tunneling through the SB can be increased, resulting in improvement of the electrical properties of the p-GaN contact.

1.4 Research Flow

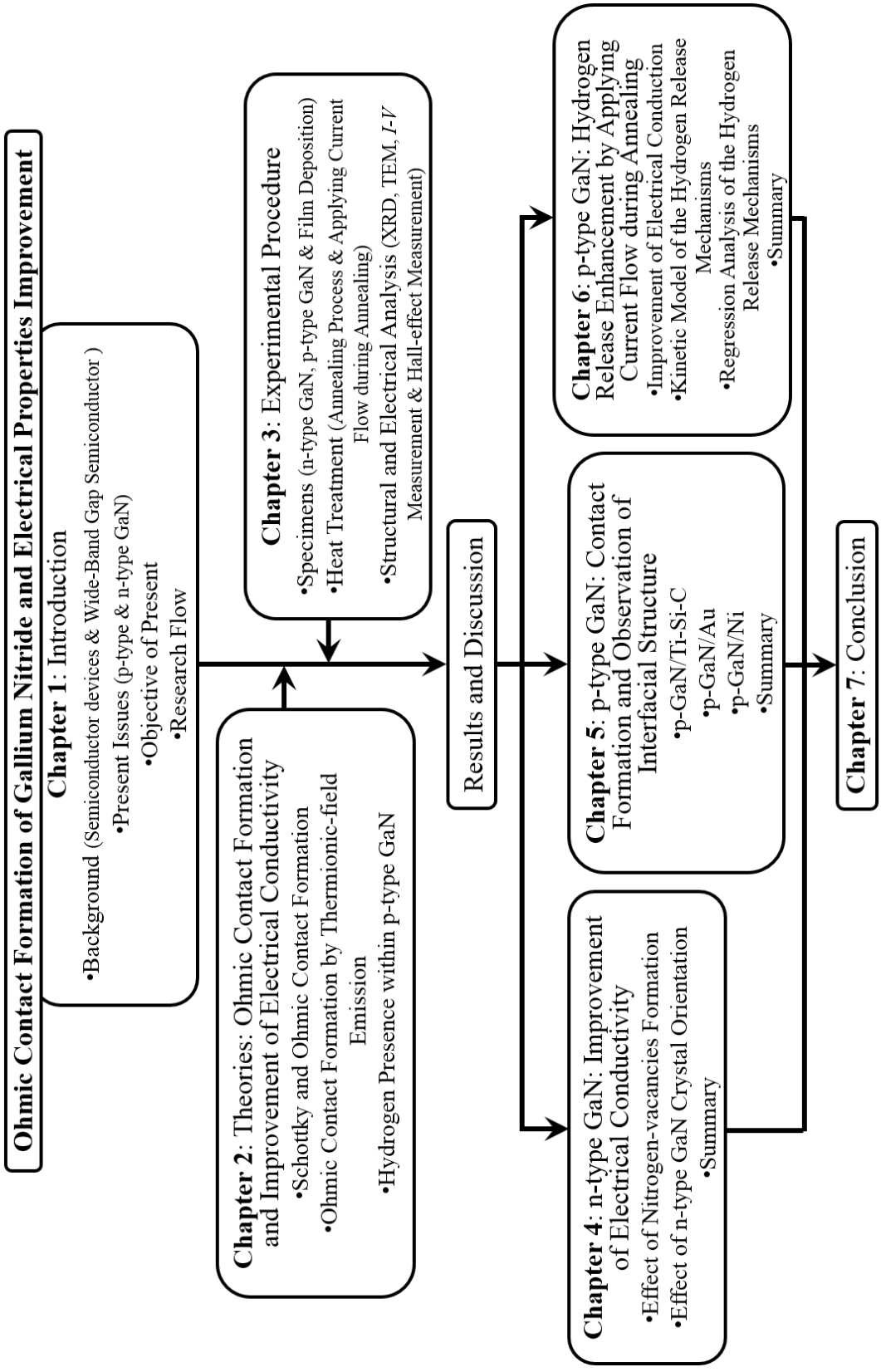

References:

[1] L D Madsen, "Formation of ohmic contacts to α-SiC and their impact on devices," Journal of Electronic Materials 30, Issue 10 (2001), 1353-1360.

[2] S. Y. Davydov, "On the Electron Affinity of Silicon Carbide Polytypes," Semiconductors 41 (2007), 696-698.

[3] J. Sumakeris, Z. Sitar, K. S. Ailey-Trent, K. L. More and R. F. Davis, "Layer-by-layer epitaxial growth of GaN at low temperatures," Thin Solid Films 225 (1993), 244-249.

[4] M. Gao, S. Tsukimoto, S. H. Goss, S. P. Tumakha, T. Onishi, M. Murakami and L. J. Brillson, "Role of Interface Layers and Localized States in TiAl-Based Ohmic Contacts to p-Type 4H-SiC," Journal of Electronic Materials 36 (2007), 277-284.

[5] H. Okumura, K. Ohta, K. Ando, W. W. Rühle, T. Nagatomo and S. Yoshida, "Bandgap energy of cubic GaN," Solid-State Electronics 41 (1997), 201-204.

[6] J. Crofton, L. Beyer, J. R. Williams, E. D. Luckowski, S. E. Mohney and J. M. Delucca, "Titanium and aluminum-titanium ohmic contacts to p-type SiC," Solid-State Electronics 41(1997), 1725-1729.

[7] B. J. Johnson and M. A. Capano, "Mechanism of ohmic behavior of Al/Ti contacts to p-type 4H-SiC after annealing," Journal of Applied Physics 95 (2004), 5616-5620.

[8] S. Tsukimoto, K. Nitta, T. Sakai, M. Moriyama and M. Murakami, "Correlation between the electrical properties and the interfacial microstructures of TiAl-based ohmic contacts to p-type 4H-SiC," Journal of Electronic Materials 33 (2004), 460-466.

[9] B. Veisz and B. Pécz, "Polarity dependent Al–Ti contacts to 6H–SiC," Applied Surface Science 233 (2004), 360-365.

[10] S. Tsukimoto, K. Ito, Z. Wang, M. Saito, Y. Ikuhara and M. Murakami, "Growth and Microstructure of Epitaxial Ti_3SiC_2 Contact Layers on SiC," Materials Transactions 50 (2009), 1071-1075.

[11] M. Maeda, K. Nonomura, Y. Takahashi and K. Tenyama, 2007 Proc. 8th Int. Conf. on Brazing, High Temperature Brazing and Diffusion Welding (LÖT 2007) (Aachen, Germany, June 2007) (Düsseldorf, Germany: DVS Verlag), 84-87.

[12] M. Maeda, T. Yamasaki and T. Takahashi, "Ohmic Contact Mechanism of Titanium-based electrodes on n-type Gallium Nitride," Transactions of JWRI 41 (2012), 45-48.

[13] H. W. Jang and J.-L. Lee, "Low-resistance and high-reflectance Ni/Ag/Ru/Ni/Au ohmic contact on p-type GaN," Applied Physics Letter 85 (2004), 4421-4423.

[14] L.-C. Chen, J.-K. Ho, C.-S. Jong, C. C. Chiu, K.-K. Shih, F.-R. Chen, J.-J. Kai and L. Chang, "Oxidized Ni/Pt and Ni/Au ohmic contacts to p-type GaN," Applied Physics Letters 76 (2000), 3703-3705.

[15] S. Nakamura, T. Mukai, M. Senoh and N. Iwasa, "Thermal Annealing Effects on P-Type Mg-Doped GaN Films," Japanese Journal of Applied Physics 31 (1992), L139- L142.

[16] S. Nakamura, M. Senoh and T. Mukai, "Highly P-Typed Mg-Doped GaN Films Grown with GaN Buffer Layers," Japanese Journal of Applied Physics 30 (1991), L1708-L1711.

[17] H. Amano, M. Kito, K. Hiramatsu and I. Akasaki, “P-Type Conduction in Mg-Doped GaN Treated with Low-Energy Electron Beam Irradiation (LEEBI),” Japanese Journal of Applied Physics 28 (1989), L2112-L2114.

[18] R. Piotrzkowski, E. Litwin-Staszewska, T. Suski and I. Grzegory, “Study of dopant activation in bulk GaN: Mg,” Physica B 308-310 (2001) 47-50.

[19] E. Litwin-Staszewska, T. Suski, R. Piotrzkowski, I. Grzegory, M.Bockowski, J. L. Robert, L. Konczewicz, D. Wasik, E. Kaminska, D.Cote and B. Clerjaud, “Temperature dependence of electrical properties of gallium-nitride bulk single crystals doped with Mg and their evolution with annealing,” Journal of Applied Physics 89 (2001), 7960-7965.

[20] S. J. Pearton, J. C. Zolper, R. J. Shul, and F. Ren, “GaN: Processing, defects, and devices,” Journal of Applied Physics 86, No. 1 (1999), 1-78.

[21] S. Nakamura, N. Iwasa, M. Senoh, and T. Mukai, “Hole Compensation Mechanism of P-Type GaN Films,” Japanese Journal of Applied Physics 31 (1992), 1258-1266.

[22] J. Neugebauer and C. G. Van De Walle, “Hydrogen in GaN: Novel Aspects of a Common Impurity,” Physics Review Letters 75, No. 24 (1995), 4452-4455.

[23] B. Clerjaud, D. Cote, A. Lebkiri, C. Naud, J. M. Baranowski, K. Pakula, D. Wasik, and T. Suski, “Infrared spectroscopy of Mg-H local vibrational mode in GaN with polarized light,” Physical Review B 61, No. 12 (2000), 8238-8241.

[24] S. M. Myers, C. H. Seager, A. F. Wright, B. L. Vaandrager, and J. S. Nelson, “Electron-beam dissociation of the MgH complex in p-type GaN,” Journal of Applied Physics 92, No. 11 (2002), 6630-6635.

[25] M. S. Myers and A. F. Wright, M. Sanati and S. K. Estreicher,“Theoretical properties of the N vacancy in p-type GaN(Mg,H) at elevated temperatures,” Journal of Applied Physics 99 (2006), 113506 1-12.

[26] S N Mohammad, “Contact mechanisms and design principles for alloyed ohmic contacts to n-GaN,” Journal of Applied Physics 95 (2004), 7940-7953.

[27] I. Fujimoto, H. Asamizu, M. Shimada, M. Moriyama, N. Shibata and M. Murakami, “Effects of vacuum annealing on electrical properties of GaN contacts,” Journal of Electronic Materials 32 (2003), 957-963.

[28] D. C. Look, D. C. Reynolds, J. W. Hemsky, J. R. Sizelove, R. L. Jones, and R. J. Molnar, “Defect Donor and Acceptor in GaN,” Physical Review Letters 79 (1997), 2273-2276.

[29] B. P. Luther, S. E. Mohney and T. N. Jackson, “Titanium and titanium nitride contacts to n-type gallium nitride,” Semiconductor Science and Technology 13 (1998), 1322-1327.

[30] Z. Fan, S. N. Mohammad, W. Kim, Ö. Aktas, A. E. Botchkarev and H. Morkoç, “Very low resistance multilayer Ohmic contact to n-GaN,” Applied Physics Letters 68 (1996), 1672-1674.

[31] L. L. Smith, R. F. Davis, R-J. Liu, M. J. Kim and R. W. Carpenter, “Microstructure, electrical properties, and thermal stability of Ti-based ohmic contacts to n-GaN,” Journal of Materials Research 14 (1999), 1032-1038.

[32] M. Maeda and Y. Takahashi, “Control of interfacial properties in power electronic devices,” International Journal of Nanotechnology (IJNT) 10 (2013), 89-99.

[33] M. Maeda, T. Yamasaki and Y. Takahashi, “Effect of interfacial reaction on electrical conduction across the interface between n-type gallium nitride and contact materials,” Journal of Physics: Conference Series 379 (2012), 012020 1-8.

Chapter 2: Theories: Ohmic Contact Formation and Improvement of Electrical Conductivity

2.1 Schottky and Ohmic Contact Formation

The simple mechanism of Schottky and ohmic contact formation of p-type GaN are illustrated in Fig. 2.1 and Fig. 2.2, respectively. The band structures in the case when the value of the work function of the metal material (Φ_m) is smaller than the total value of electron affinity (χ) and bandgap energy (E_g) of the p-type semiconductor are illustrated in Fig 2.1 (a). When these to materials are connected, due to the Fermi level of the metal (E_{FM}) is lower than the Fermi level of the p-type semiconductor (E_F), the carriers will flow from the p-type semiconductor side into the metal side. As the result, the up-bending of the bandgap energy of the p-type semiconductor will occur at the contact interface. These phenomena will lead to the equalization of the Fermi level of these two materials as shown in Fig. 2.1 (b). In this case, a depleted zone of carriers (holes) will be formed at the contact interface between metal and semiconductor. This depleted zone will cause the interference of carrier transportation across the contact interface. This interference zone is known as Schottky barrier. Carriers moving across such a contact interface require energy to get over the barrier. Thus, Joule heat is generated at the interface, which deteriorates the energy efficiency and the reliability of the device.

The band structures in the case when the value of work function of the metal material (Φ_m) is equal or greater than the total value of electron affinity (χ) and the bandgap energy (E_g) of the p-type semiconductor are illustrated in Fig. 2.2 (a). When these two types of materials are connected, due to the Fermi level of the metal (E_{FM}) is

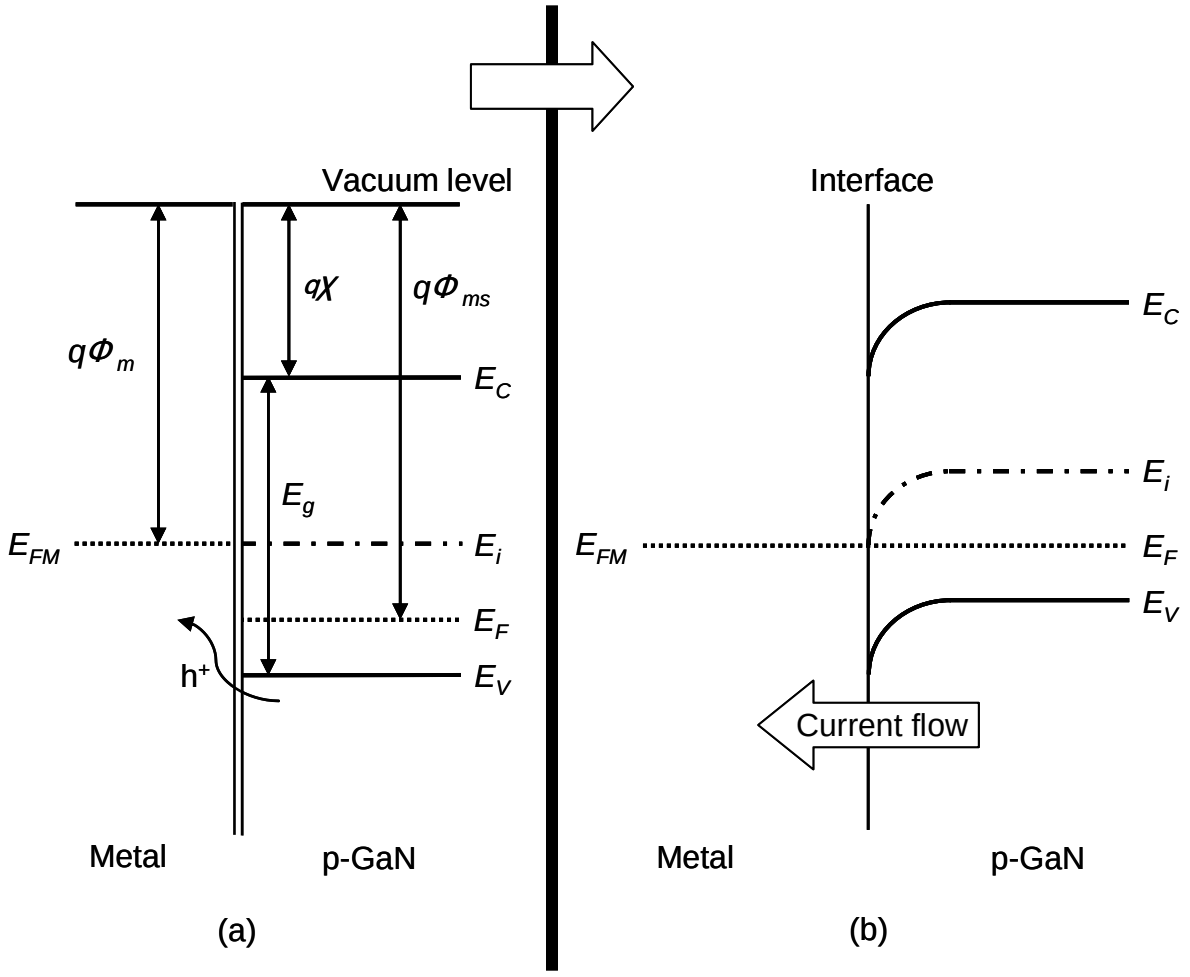

Fig. 2.1 Typical Schottky contact p-type GaN.

higher than the Fermi level of the p-type semiconductor (E_F), the carriers will flow from the metal side into the p-type semiconductor side. As the result, with the similar idea used in the Schottky contact, down-bending of the bandgap energy of the p-type semiconductor will occur at the contact interface. These phenomena will lead to the equalization of Fermi level of these two materials as shown in Fig. 2.2 (b). Due to no formation of barrier occurring at the contact interface, the carriers can move freely across the contact interface between the metal and the p-type semiconductor. Ohmic contact formed when the carriers flow over the lowed barrier is also known as ohmic contact formation by thermionic emission.

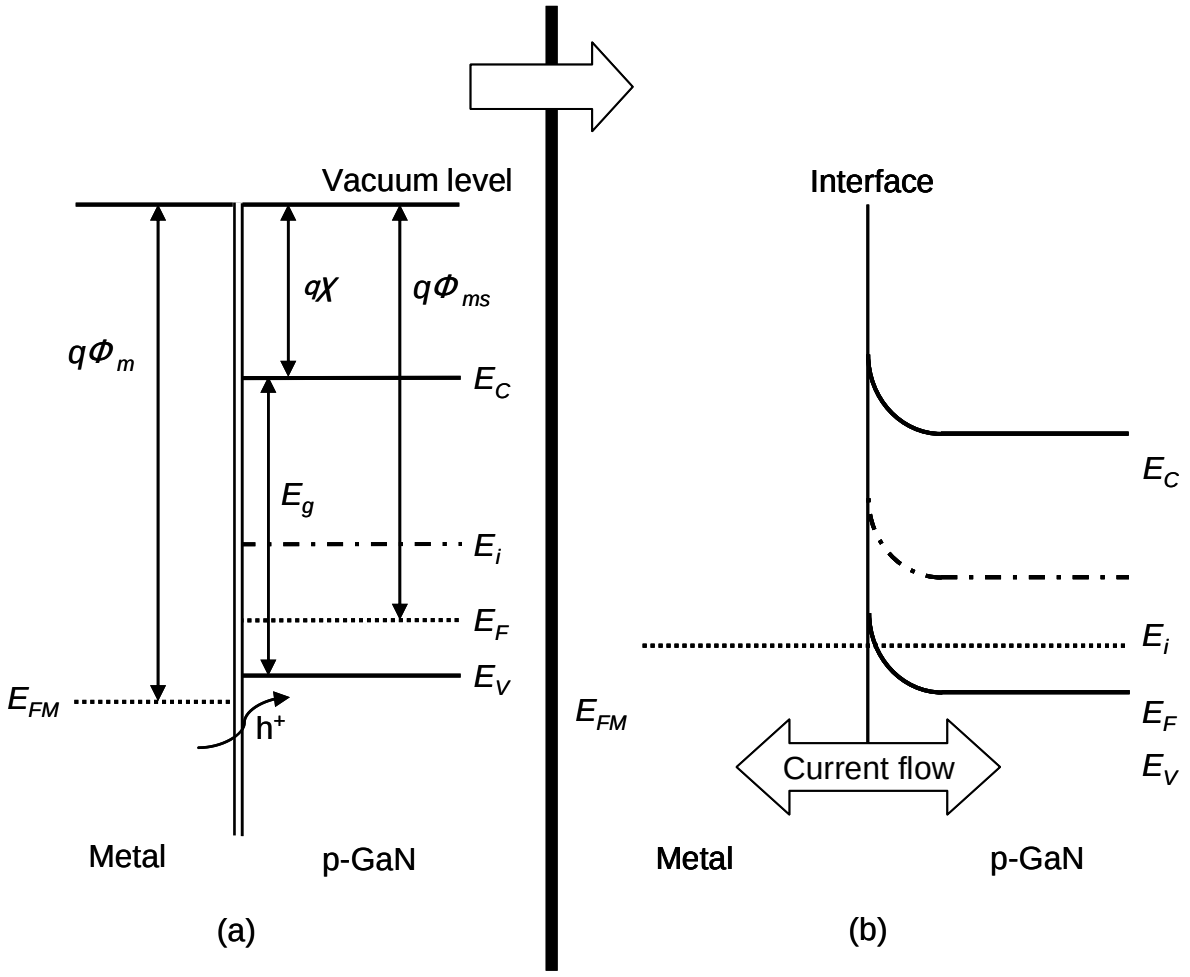

Fig. 2.2 Typical Ohmic contact p-type GaN.

2.2 Ohmic Contact Formation by Thermionic-field Emission

If ohmic formation only can be form by thermionic emission as discussed above, the ohmic contact formation of wide band-gap semiconductor such as GaN would be very difficult. For example, contact materials with work function higher than 7.50 eV is need to form ohmic contact with p-type GaN. However, there are two others mechanisms of carrier conduction between metal and semiconductor, which are thermionic-field emission and field emission. Thermionic emission occurs when some fraction of the carriers have enough thermal energy to overcome the barrier and cross the junction. On

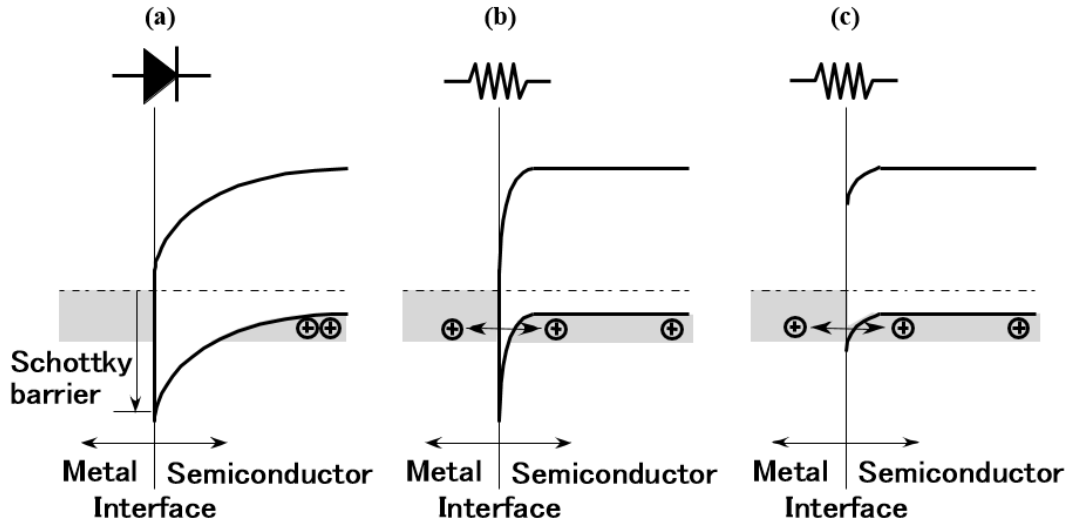

Fig. 2.3 Band structure between metal and p-type semiconductor. (a) Schottky contact, (b) Ohmic contact formation by field emission and (c) Ohmic contact formation by thermionic-field emission.

the other hand, field emission or also known as tunneling is a quantum-mechanical process when a carrier crossing a barrier despite having insufficient energy to go over it. The tunneling phenomena is strongly dependent on barrier width. The ohmic formation by these two mechanisms are illustrated in the Fig. 2.3. In the Fig. 2.3 (b), by heavily doping the semiconductor, barrier width is significantly narrowed and ohmic contact can be achieved. However, by heavily-dope a semiconductor, high level of impurities will be introduced to the semiconductor crystalline. This impurities will leads to growth disturbances such as stacking faults, which consequently degrade the quality of crystalline.

As shown in Fig. 2.3 (c), ohmic contact can also be formed by thermionic-field emission, which combining both lowering the height and narrowing the width of the barrier. For wide band-gap semiconductor such as GaN, this mechanism of ohmic formation seem to be the best method. By using a contact materials with high work function such as Ni (5.1 eV), the barrier can be lowed to certain degree. Then, by further

improve the carrier concentration, the ohmic contact by thermionic-field emission can be formed.

2.3 Hydrogen Presence within p-type GaN

In the case of p-type GaN, due to the energy level of Mg-acceptor is very deep, it is known that only one percent of doped-Mg can be activated and work as carrier. Therefore, it is difficult to achieve a considerable high carrier concentration of p-type GaN. For example, to attain p-type GaN with carrier concentration in order 10^{17} cm^{-3}, it is necessary to incorporate extremely high dopant concentration (10^{19} cm^{-3}) into GaN. This high level of impurities will leads to growth disturbances such as stacking faults, which consequently degrade the quality of GaN crystalline.

Additionally, the presence of hydrogen (H) in GaN, which incorporated during the GaN growth process, further reduce the carrier concentration of p-type GaN. H is known to electrically passivate the acceptors [1]. This passivation is attributed to the

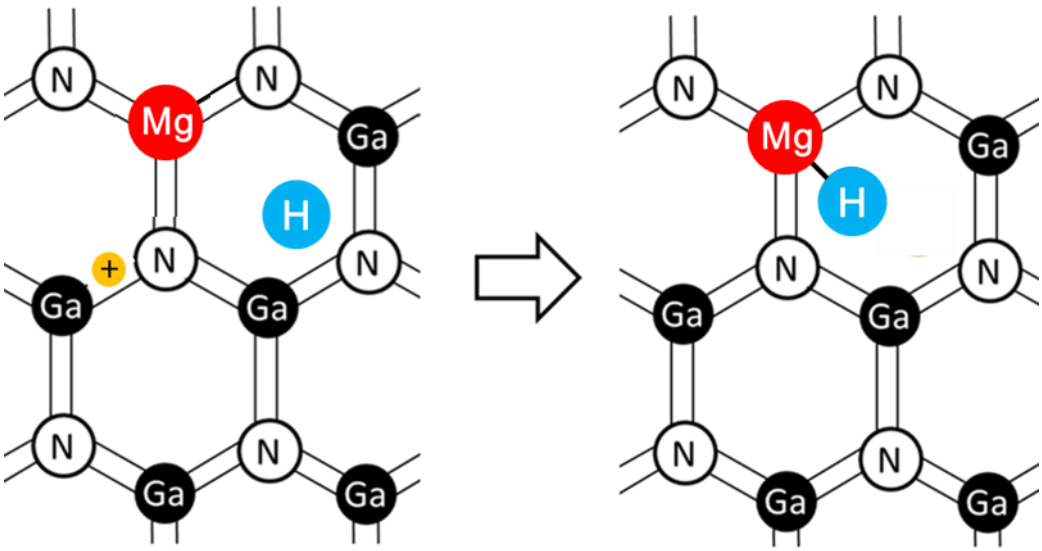

Fig. 2.4 Symmetrical illustrations of Mg-H complex formation with p-type GaN.

formations of neutral Mg-H complexes where H is bonded interstitially to a neighboring nitrogen atom [2-4], as illustrated if Fig. 2.4. Therefore, in order to achieve p-type conductivity, postgrowth activation of Mg by thermal annealing, which releases H from GaN, is necessary [5]. However, the thermal annealing is believed to releases H from GaN but not so effective.

Moreover, numerous investigations of p-type GaN have suggested that the elevated temperature during the contact formation process can cause development of N-vacancies within GaN sub-surface, which consequently reduce the hole concentration of the p-type GaN [6]. As shown in Fig, 2.5, under a high temperature, GaN has a high tendency to decompose into Ga and N. This decomposition will lead to the formation of N-vacancies within GaN. These vacancies are known to act as n-type dopant atoms with

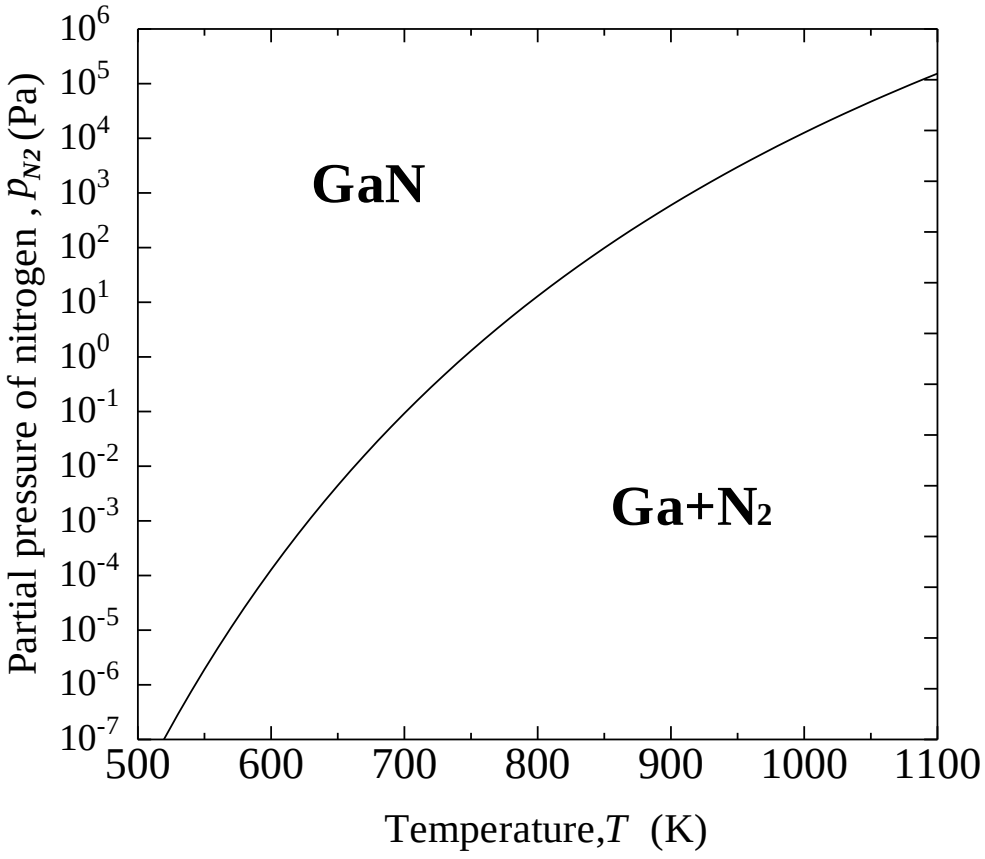

Fig. 2.5 Temperature dependence of equilibrium partial pressure of nitrogen.

a donor level very close to the conduction band edge of n-type GaN [7]. Fujimoto et al. reported that Hall-effect measurements revealed that an n-type conductive layer was formed near the p-GaN surfaces by annealing at 1073 K in vacuum [8]. Therefore, it is important to understand and improve the processes of H release from p-GaN and contact formation under lower temperature conditions.

Reference:

[1] S. Nakamura, N. Iwasa, M. Senoh, and T. Mukai, "Hole Compensation Mechanism of P-Type GaN Films," Japanese Journal of Applied Physics 31 (1992), 1258-1266.

[2] J. Neugebauer and C. G. Van De Walle, "Hydrogen in GaN: Novel Aspects of a Common Impurity," Physics Review Letters 75, No. 24 (1995), 4452-4455.

[3] B. Clerjaud, D. Cote, A. Lebkiri, C. Naud, J. M. Baranowski, K. Pakula, D. Wasik, and T. Suski, "Infrared spectroscopy of Mg-H local vibrational mode in GaN with polarized light," Physical Review B 61, No. 12 (2000), 8238-8241.

[4] S. M. Myers, C. H. Seager, A. F. Wright, B. L. Vaandrager, and J. S. Nelson, "Electron-beam dissociation of the MgH complex in p-type GaN," Journal of Applied Physics 92, No. 11 (2002), 6630-6635.

[5] S. Nakamura, T. Mukai, M. Senoh and N. Iwasa, "Thermal Annealing Effects on P-Type Mg-Doped GaN Films," Japanese Journal of Applied Physics 31 (1992), L139- L142.

[6] M. S. Myers and A. F. Wright, M. Sanati and S. K. Estreicher,"Theoretical properties of the N vacancy in p-type GaN(Mg,H) at elevated temperatures," Journal of Applied Physics 99 (2006), 113506 1-12.

[7] S N Mohammad, “Contact mechanisms and design principles for alloyed ohmic contacts to n-GaN,” Journal of Applied Physics 95 (2004), 7940-7953.

[8] I. Fujimoto, H. Asamizu, M. Shimada, M. Moriyama, N. Shibata and M. Murakami, “Effects of vacuum annealing on electrical properties of GaN contacts,” Journal of Electronic Materials 32 (2003), 957-963.

Chapter 3: Experimental Procedure

In this chapter, the experimental procedure used in present study which is including specimens (gallium nitride substrate and contact materials), films deposition, heat treatment and structural and electrical analysis will be explained.

3.1 Specimens

3.1.1 n-type GaN

The n-type GaN substrates used in the present study were 2.3-μm-thick, 50.8-mm-diameter wafer of n-type GaN epitaxially grown on a 330.0-μm-thick sapphire (0001) wafer with a 2.1-μm-thick GaN buffer layer. The surface orientations and carrier

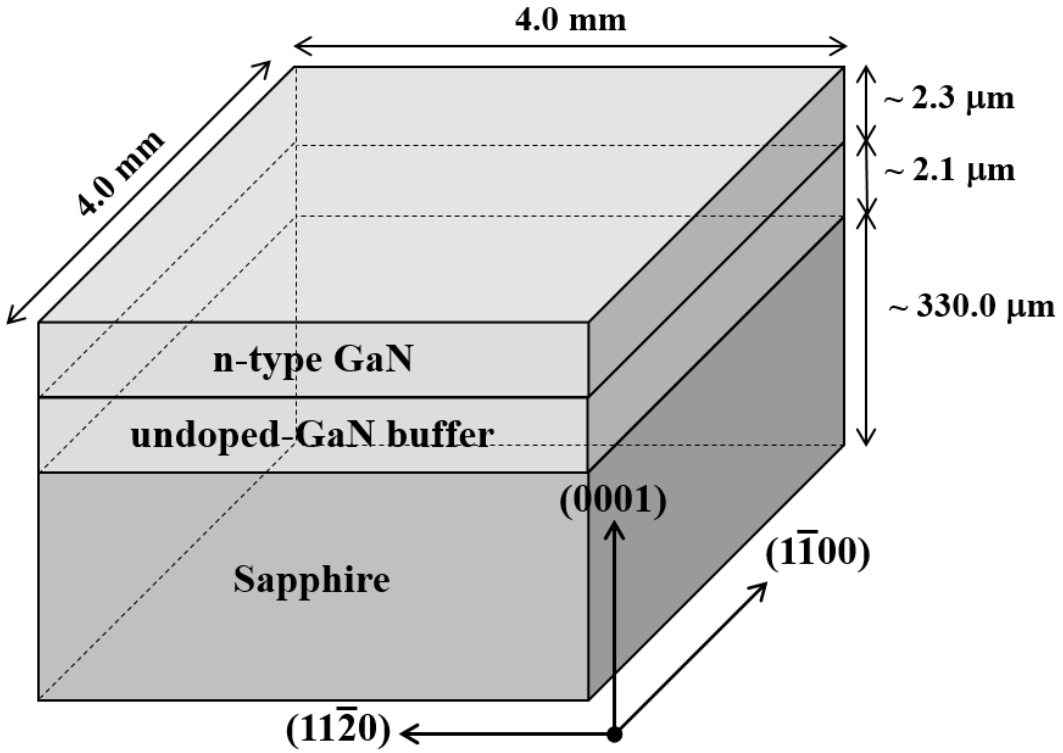

Fig. 3.1 Dimension of n-type GaN substrate.

density of the substrate were (0001) Ga-face and 4×10^{18} cm^{-3}, respectively. The wafer was then cut into 4.0-mm-squares using an automatic dicing machine. The dimension of the substrate is shown in Fig. 3.1. Additionally, to compare the properties of n-type GaN contact on variety of surface orientations, three different surface orientations of GaN were used: $(000\bar{1})$ N-face, $(10\bar{1}0)$ and $(11\bar{2}0)$.

3.1.2 p-type GaN

The p-type GaN substrates used in the present study were 2.0-μm-thick, 50.8-mm-diameter wafer of p-type GaN epitaxially grown on a 330.0-μm-thick sapphire (0001) wafer with a 2.4-μm-thick GaN buffer layer. The surface orientation and carrier density of the substrate were (0001) Ga-face and 3×10^{17} cm^{-3}, respectively. The wafer was then cut into 4.0-mm-square using the automatic dicing machine. The dimension of the substrate is shown in Fig. 3.2.

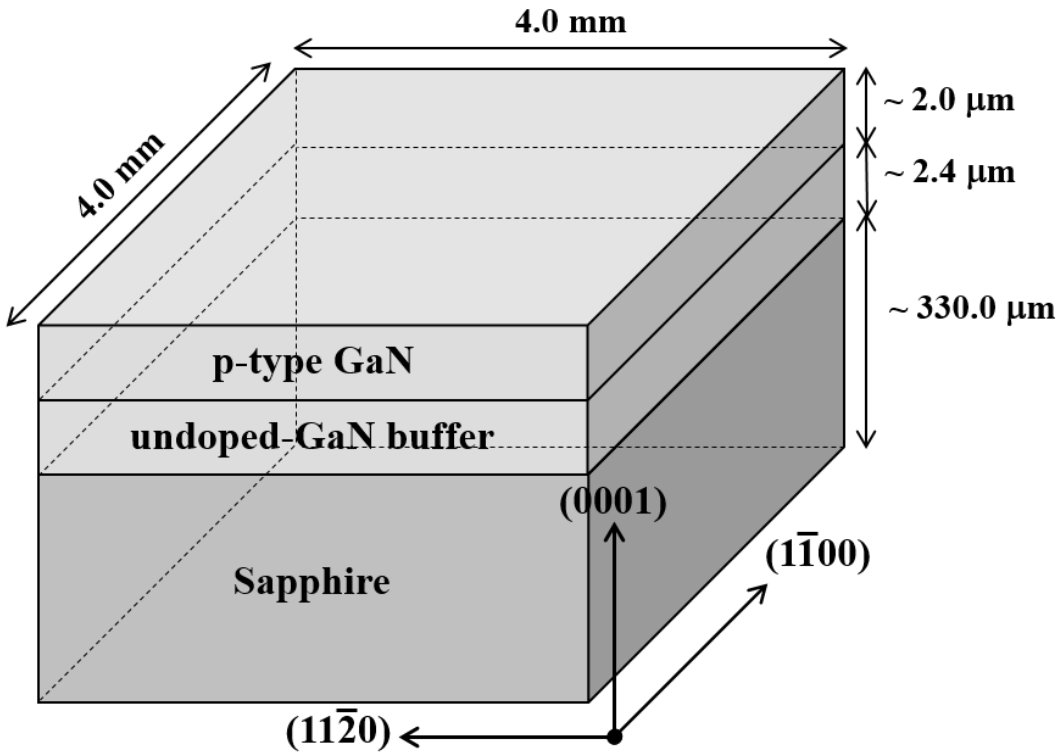

Fig. 3.2 Dimension of p-type GaN substrate.

3.1.3 Film Deposition

Sputtering Depositions

In present study, the radio-frequency (RF) magnetron sputtering deposition method was used for film deposition on the GaN substrates. The RF magnetron sputtering apparatus has a configuration schematically illustrated in Fig. 3.3. Before the deposition process, the substrates were cleaned with acetone applying ultrasonic vibration. Then, the substrates were fixed in the RF magnetron sputter deposition apparatus. Before the sputter deposition, the surfaces of targets and the substrates were sputter-cleaned. Sputter-cleaning were performed in 8 Pa of 99.9999% Ar under the RF power of 200 W for 300 s. The sputter deposition films on the substrates were performed immediately after the sputter-cleaning. The sputter deposition conditions for each film materials were shown in Table 3.1. The dimension of specimens after the deposition process is illustrated in Fig 3.4 and Fig. 3.5.

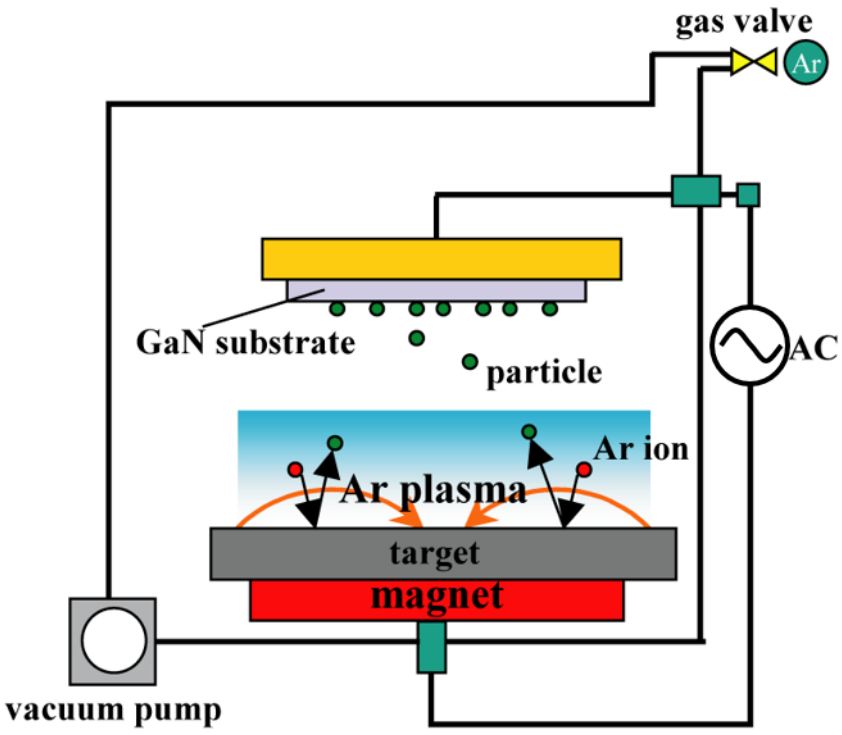

Fig. 3.3 Schematic illustration of RF magnetron sputtering apparatus.

Table 3.1 Sputter deposition conditions for film materials.

Specimen	Deposited Film	Sputter Time [s]	Ar Pressure [Pa]	RF Power [W]
n-type GaN	Ti	600	8	200
p-type GaN	$Ti_{49}Si_{18}C_{33}$ [at. %]	600	0.8	200
	Au	36	8	100
	Ni	1800	20	200
	Pd	27	8	100

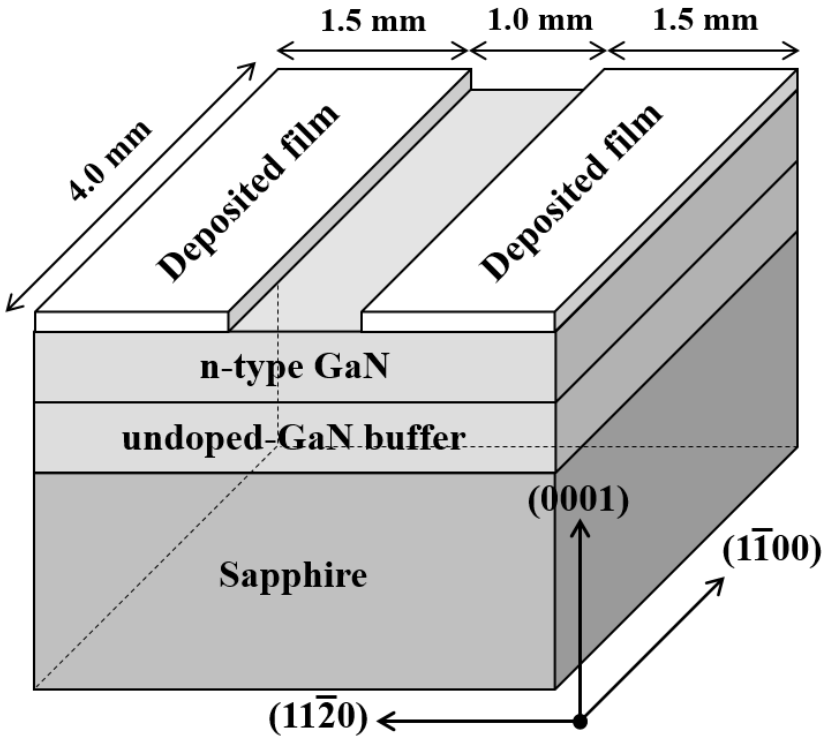

Fig. 3.4 Dimension of n-type GaN specimens after deposition process.

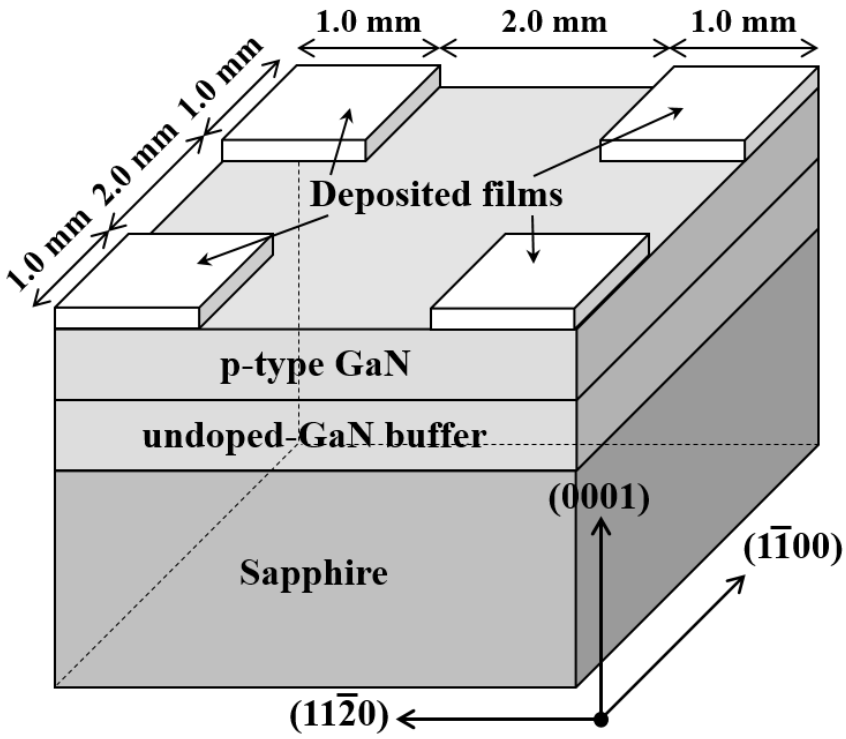

Fig. 3.5 Dimension of p-type GaN specimens after deposition process.

Electron Probe Micro-Analyzer (EPMA)

In the present study, EPMA was used to verify the composition of deposited films. EPMA is fundamentally the same as a Scanning Electron Microscopy (SEM), with the added capability of chemical analysis. The primary importance of an EPMA is the ability to acquire precise, quantitative elemental analyses at very small "spot" sizes, primarily by wavelength-dispersive spectroscopy (WDS).

An electron microprobe operates under the principle that if a solid material is bombarded by an accelerated and focused electron beam, the incident electron beam has sufficient energy to liberate both matter and energy from the specimen. These electron-specimen interactions mainly liberate heat, but they also yield both derivative electrons and x-rays. X-ray generation is produced by inelastic collisions of the incident electrons

with electrons in the inner shells of atoms in the specimen; when an inner-shell electron is ejected from its orbit, leaving a vacancy, a higher-shell electron falls into this vacancy and must shed some energy (as an X-ray) to do so. These quantized x-rays are characteristic of the element.

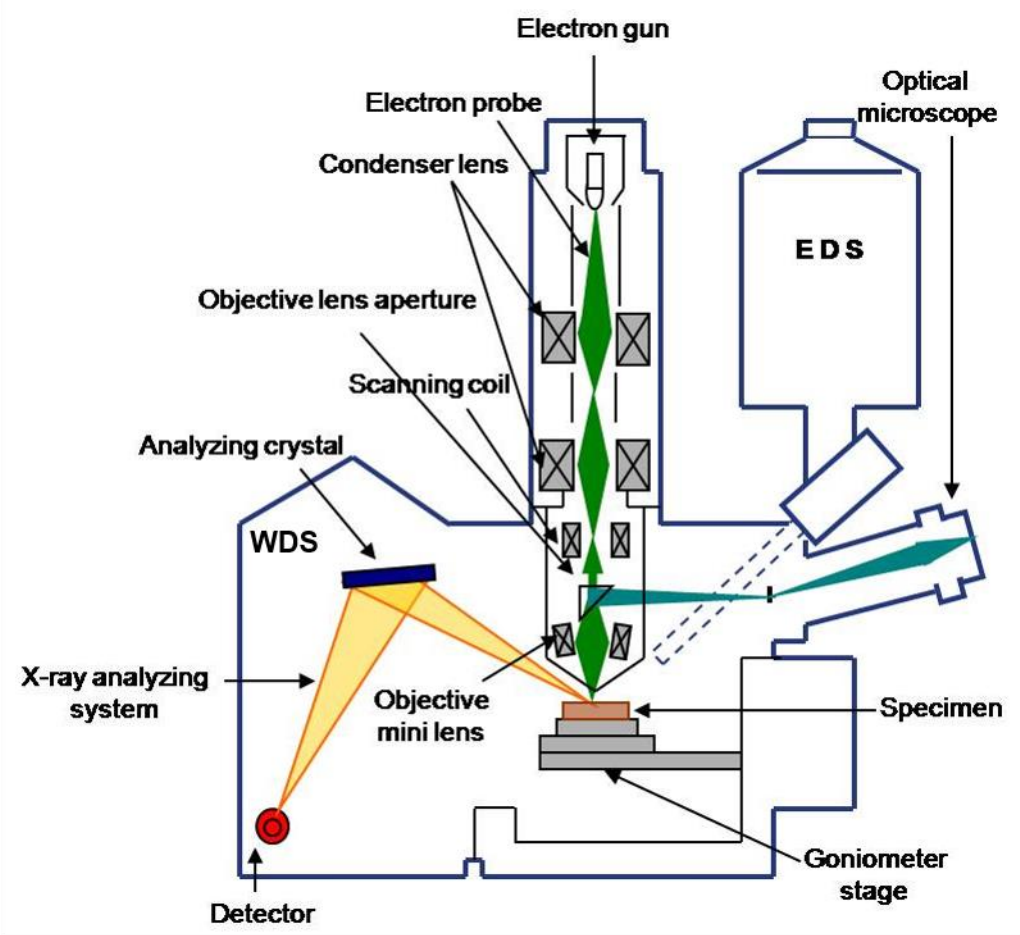

Fig. 3.6 Schematic diagram of EPMA.

3.2 Heat Treatment

3.2.1 Annealing Process

Heat treatment in the present study was carried out by using a tubular vacuum furnace as schematically illustrated in Fig. 3.7. The heat treatment conditions for each specimens were shown in Table 3.2. After the heat treatment, the specimens then were cooled down by natural cooling in the furnace until reaching the room temperature.

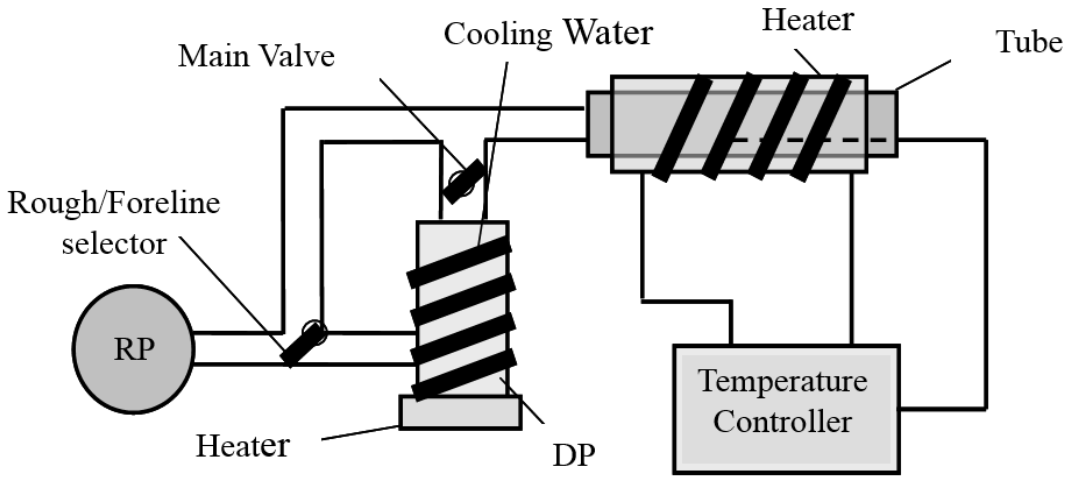

Fig. 3.7 Schematic illustration of tubular vacuum furnace.

Table 3.2 Heat treatment conditions for each specimens

Specimen	Deposited Film	Annealing Temperature [K]	Hold Time [s]	Annealing Ambient [Pa]
n-type GaN	Ti	773, 973	300	Vacuum 1.3×10^{-3}
p-type GaN	$Ti_{49}Si_{18}C_{33}$ [at. %]	973, 1073	0	Vacuum 1.3×10^{-3}
	Au	573, 673	3600	Nitrogen 1.0×10^{5}
	Ni	573, 673	3600, 9000	Nitrogen 1.0×10^{5}
	Pd	673	9000	Nitrogen 1.0×10^{5}

3.2.2 Applying Current Flow during Annealing

In the present study, some of the p-type GaN/Ni specimens were subjected current flow under the condition of DC 30 V. The schematic illustration of these methods are shown in Fig. 3.8. Additionally, to investigate the effect of applying current flow during annealing, the changes of the current values were observed for the p-type GaN/Ni and p-type GaN/Pd contacts during annealing at 673 K while subjected to current flow under the condition of 10 V. When the current was measured, the voltage was reduced from 10 V to 1.0 V. The schematic illustration of these methods are shown in Fig. 3.9.

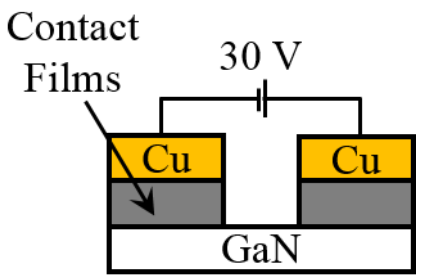

Fig. 3.8 Schematic illustration of methods and contact structures for applying current flow through specimens during annealing.

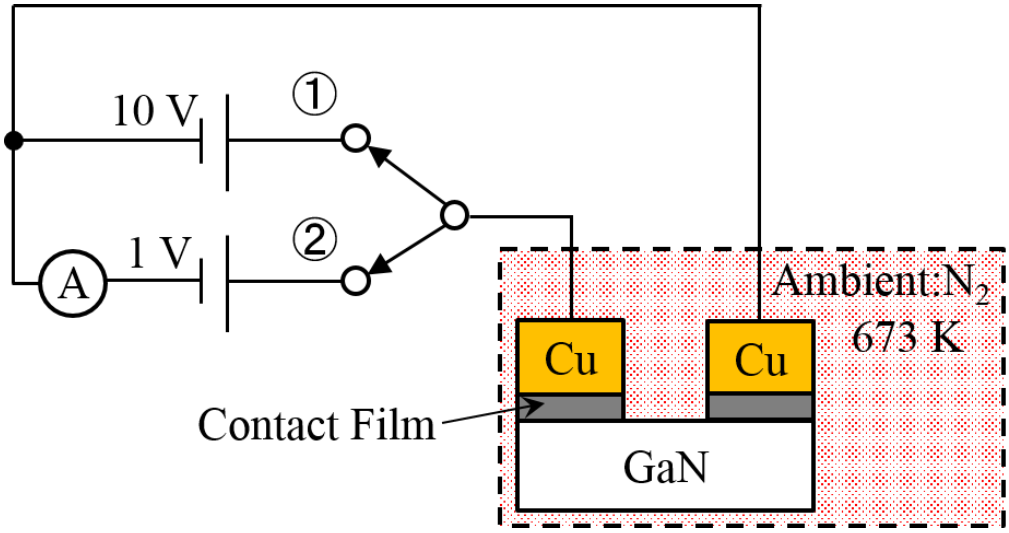

Fig. 3.9 Schematic illustration of the methods to measure changes of current values of p-type GaN/Ni and p-type GaN/Pd contacts during annealing at 673 K.

3.3 Structural and Electrical Analysis of the Contacts

3.3.1 Microstructure Observation and Phase Identification

X-ray diffraction (XRD)

In present study, the X-ray diffractometer as illustrated in Fig. 3.10 was used to analyze the structure of the as-deposited and annealed specimens. XRD is an analysis method of determining the atomic and molecular structure of a crystal, in which the crystalline atoms cause a beam of X-rays to diffract into many specific directions. An X-ray which scatters from the surface of a substance has travelled less distance than an X-ray which scatters from a plane of atoms inside the crystal. The penetrating X-ray travels down to the internal layer, reflects, and travels back over the same distance before being back at the surface. The travelling distance depends on the separation of the layers and the angles at which the X-ray entered and scatters out of the materials. This principle can be expressed in an equation known as Bragg's Law:

$$2d \sin\theta = n\lambda \tag{3.1}$$

where d, θ and λ are the spacing between layers of atoms, angle of the incident rays from the surface of the crystal and wavelength of the rays, respectively. When n is an integer (1, 2, 3 etc), the reflected waves from different layers matches perfectly in phase with each other.

In the present study, a CuKα ray source (λ = 1.540562 Å) was used, and the measurement have been done in the range of 10° to 90°. The tube voltage and tube current during the measurement process is 40kV and 40mA, respectively. The measurement methods used in the present study is θ–2θ. In this method a point detector and specimen are moved so that the detector is always at 2θ and the specimen surface is always at θ to the incident X-ray beam. This measurement method provides the best result to indentify the parallel atomic plane to the specimen surface. The other measurement conditions of XRD in the present study are shown in Table 3.3.

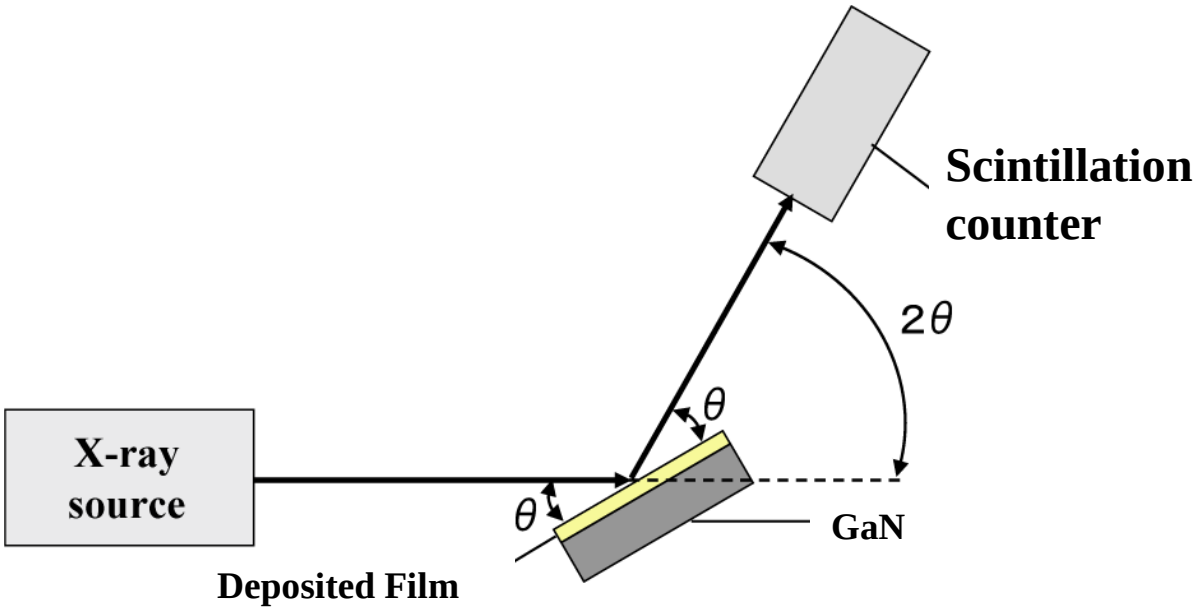

Fig. 3.10 Schematic illustration of goniometry in 2θ-θ X-ray diffractometer.

Table 3.3 Measurement conditions of XRD.

Method	$\theta-2\theta$
X-ray source	CuKa (1=1.540562Å)
Step angle [°]	0.02
Counting time [s]	0.50
Tube voltage [kV]	40.0
Tube current [mA]	40.0
Divergence slit [°]	1
Scattered slit [°]	0.5
Receiving slit [°]	0.15

Transmission electron microscopy (TEM)

The transmission electron microscope (TEM) uses a high energy electron beam transmitted through a very thin specimen to image and analyze the microstructure of materials with atomic scale resolution. The electrons are focused with electromagnetic lenses and the image is observed on a fluorescent screen, or recorded on film or digital camera. The electrons are accelerated at several hundred kV, giving wavelengths much smaller than that of light: 200kV electrons have a wavelength of 0.0025 nm. While the resolution of the optical microscope is limited by the wavelength of the illuminating light, that of the electron microscope is limited by aberrations inherent in electromagnetic lenses.

Due to the TEM specimens must be approximately 100 nm or less in thickness, the preparation of TEM specimens requires special techniques to be done. In the present

study, preparation of TEM specimens were done by focused ion beam (FIB) technique. The FIB process uses a Ga^+ ion beam with an accelerating voltage of 1-30 keV to raster over the surface of a specimen in a similar way as the electron beam in a scanning electron microscope (SEM). The secondary electrons generated by the primary ion beam give an image (ion image), which is used to control the machining process precisely. The machining procedure used in the present is shown in Fig. 3.11.

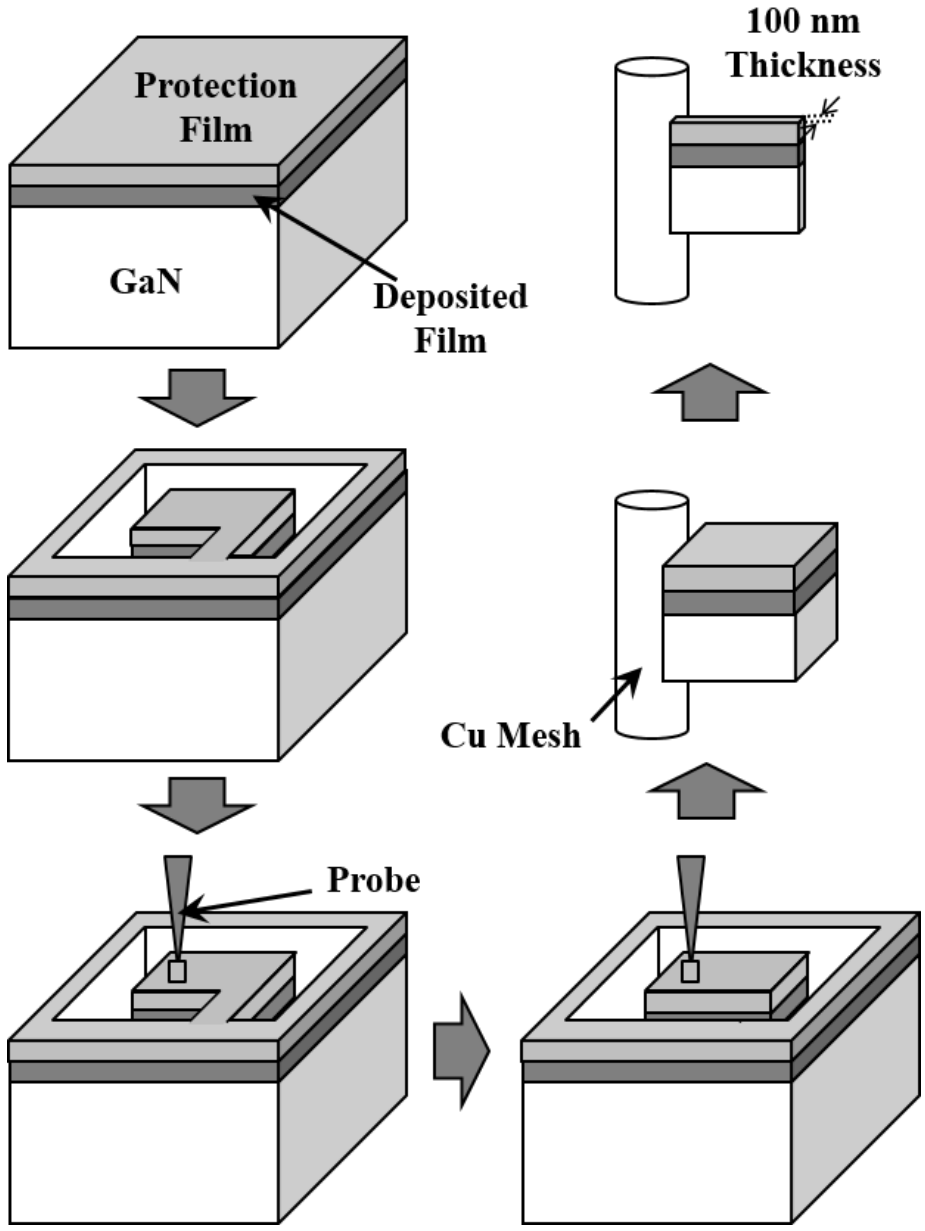

Fig. 3.11 The machining procedure of FIB process.

3.3.2 Electrical Conduction Test and Hall-Effect Measurement

I-V Measurement

The schematic diagram of electrical conduction test used in the present study is shown in the Fig. 3.12. This measurement device was consisting of a direct current (DC) power supply (to supply stable voltage and current), precision ammeter and a digital voltmeter. This device is connected to the electrodes (probes plated with hard gold). By placing the probes on the deposited films, the electrical conduction profile of each specimens have been measured between 0 V to 10 V and 0 V to -10 V.

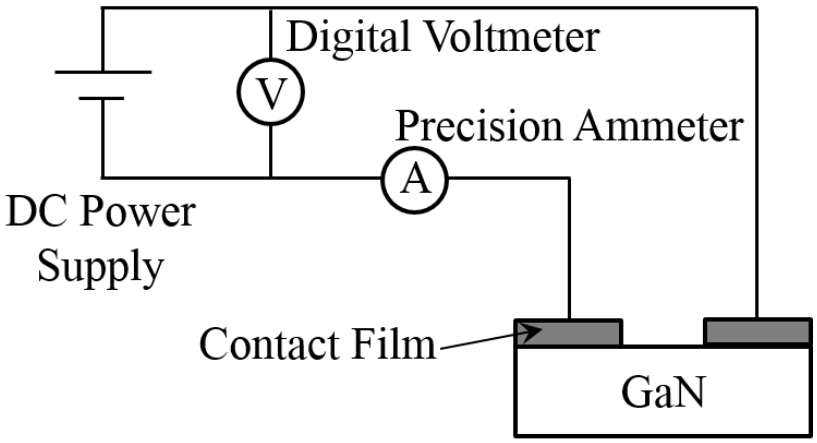

Fig. 3.12 The schematic diagram of electrical conduction test.

Hall-Effect Measurement (Van der Pauw Method)

In the present study, in order to investigate the dominant carrier-type of the p-type GaN specimens after annealing, the Hall-effect measurement tests at the room temperature were performed. The schematic diagram of Hall-effect measurement is shown in Fig. 3.13.

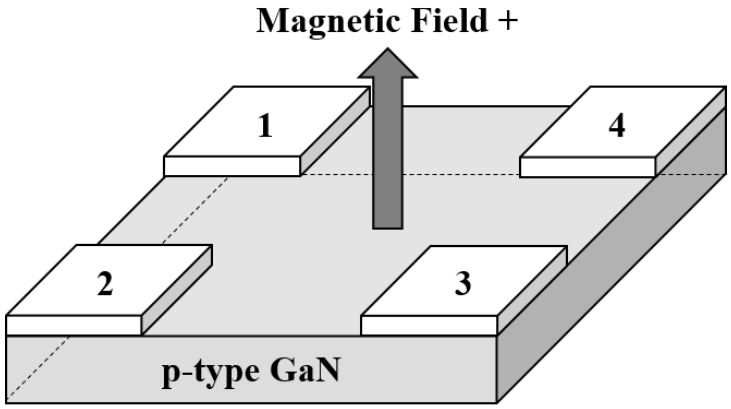

Fig. 3.13 Schematic diagram of Hall-effect measurement.

Measurement definition:

The current I_{13} is a positive DC current injected into contact 1 and taken out of contact 3, and is measured in amperes (A).

The voltage $V_{24,\,P}$ is a DC voltage measured between contacts 2 and 4 with positive magnetic field, measured in volts (V).

Injected current = constant

Magnitude of magnetic field = constant for both directions

Procedure:

Positive magnetic field:

I_{24} applied, $V_{13,P}$ measured (can be + or -)

I_{13} applied, $V_{42,P}$ measured (can be + or -)

I_{42} applied, $V_{31,P}$ measured (can be + or -)

($V_{31,P}$ should be same or suitably small degree of error with $V_{13,P}$)

I_{31} applied, $V_{24,P}$ measured (can be + or -)

($V_{24,P}$ should be same or suitably small degree of error with $V_{42,P}$)

Negative magnetic field:

I_{24} applied, $V_{13,N}$ measured (can be + or -)

I_{13} applied, $V_{42,N}$ measured (can be + or -)

I_{42} applied, $V_{31,N}$ measured (can be + or -)

($V_{31,N}$ should be same or suitably small degree of error with $V_{13,N}$)

I_{31} applied, $V_{24,P}$ measured (can be + or -)

($V_{24,N}$ should be same or suitably small degree of error with $V_{42,N}$)

Calculation:

$$V_{13} = V_{13,P} - V_{13,N} \quad (3.2)$$

$$V_{24} = V_{24,P} - V_{24,N} \quad (3.3)$$

$$V_{31} = V_{31,P} - V_{31,N} \quad (3.4)$$

$$V_{42} = V_{42,P} - V_{42,N} \quad (3.5)$$

Hall voltage is given by,

$$V_H = (V_{13} + V_{24} + V_{31} + V_{42})/8 \quad (3.6)$$

If V_H is positive; the material is p-type, if V_H is negative, the material is n-type.

Chapter 4: Results and Discussion: n-type GaN: Improvement of Electrical Conductivity

As discussed in Chapter 1 and 2, to improve the electrical conductivity of n-type GaN contacts, new effective methods to increase the formation of N-vacancies within GaN sub-surface and most suitable surface orientation of n-type GaN/Ti contact need to be determined. In this chapter, the effect of prolonging the Ar ion irradiation times during the sputtering process to form N-Vacancies within GaN sub-surface will be discussed. The Ar ion irradiation times are to be referred as (300 ~ 3600 s Ar). Additionally, the effect of different surface orientation of n-type GaN contacts and annealing conditions to electrical conductivity of the n-type GaN/Ti contact will be discussed.

4.1 Effect of Nitrogen-vacancies Formation

Fig. 4.1 shows the microstructure of the n-type GaN/Ti (300 s Ar) specimen after the Ti deposition. In the bright-field image shown in Fig. 4.1 (a), a layer of approximately 12-nm-thickness is observed adjacent to GaN substrate. Fig. 4.1 (b) shows the electron diffraction pattern taken from this area. The diffraction pattern consists of net patterns of GaN and Ti_2N. Fig. 4.1 (c) shows the dark-field image of the same area taken by using the Ti_2N 020 diffraction as mark in Fig. 4.1 (b). The image shows that only the layer adjacent to GaN substrate appears bright. Thus, it is concluded that a layer of Ti_2N is formed adjacent to GaN substrate by the Ti deposition on the GaN substrate. The N constituting Ti_2N formations are originated only from the GaN substrate. So it is likely that a huge amount of N-vacancies is formed within the GaN sub-surface closed to the contact interface.

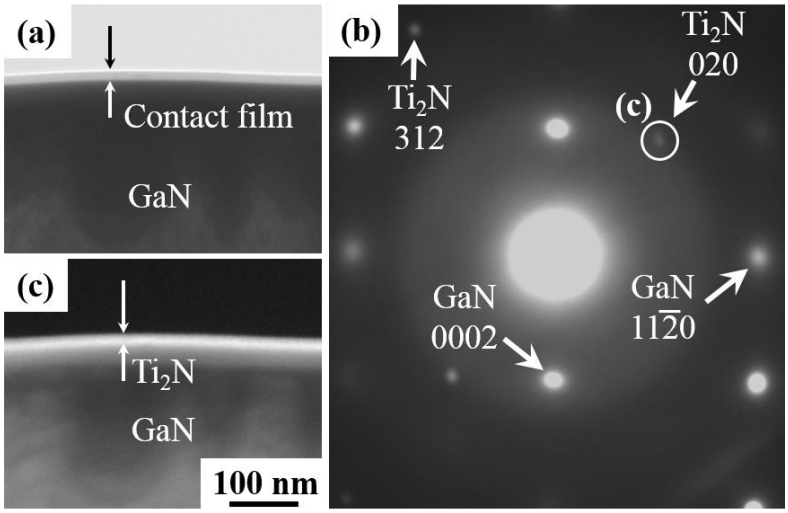

Fig. 4.1 Microstructure of n-type GaN/Ti (300 s Ar) contact without annealing. (a) bright-field image, (b) selected-area electron diffraction pattern corresponding to area shown in (a), (c) dark-field image of same area shown in (a) using Ti_2N 020 diffraction [1].

Fig. 4.2 shows the DC current-voltage (*I-V*) profiles of the specimens. The *I-V* profile of n-type GaN/Ti (300 s Ar) indicates that ohmic contacts are achieved by the Ti_2N formation during the Ti deposition and/or by Ar ion irradiation during sputtering process. Theoretically, Ti_2N is not an adequate materials for ohmic formation of n-type GaN due to its high work function. However, the results indicates that even with a Schottky barrier formed at the interface, the formation of Ti_2N and/or Ar ion irradiation has induced a sufficient amount of N-vacancies within the GaN sub-surface to make the barrier thin enough to achieve ohmic conduction. The *I-V* profile of undoped GaN/Ti (300 s Ar) contact as shown in Fig. 4.2 also complies with this result. Even with a very low initial carrier density, due to no dopant implantation, the Ti_2N formation and/or Ar ion irradiation induced sufficient amount of N-vacancies and carrier density to achieve ohmic conduction. The low electrical conductivity of undoped GaN/Ti contact is attributed to the high specific resistance of undoped GaN substrate.

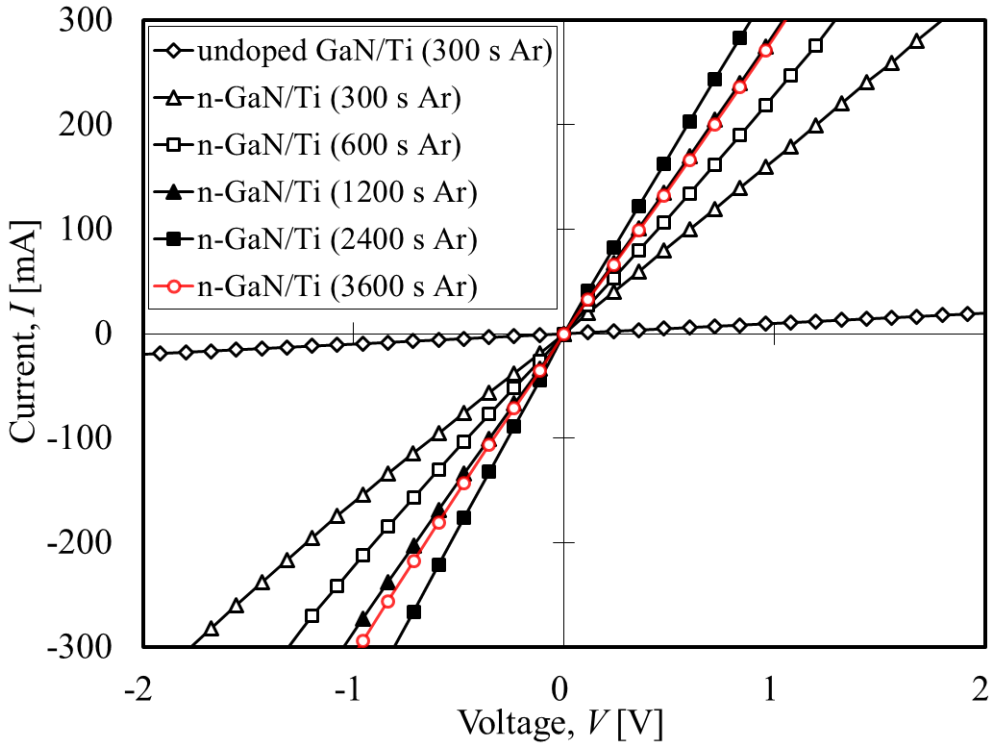

Fig. 4.2 *I-V* conduction profiles of as-deposited specimens [1].

As shown in Fig. 4.2, the effect prolonging the Ar ion irradiation time can be seen in the *I-V* profiles of n-type GaN/Ti contacts. All the *I-V* profiles except for specimen subjected to 3600 s Ar ion irradiation time indicates that ohmic conduction is achieved. Additionally, the *I-V* profile shows that longer Ar ion irradiation time resulting to higher electrical conductivity. It is suggested from this result that the amount of N-vacancies formation within the GaN sub-surface are depending to the Ar ion irradiation time. However, the *I-V* profile of specimen with 3600 s Ar ion irradiation shows no further improvement compared to specimen with 2400 s Ar ion irradiation time. This is likely due to the selective sputtering of N atoms from GaN substrate. This selective sputtering induces the phase transformation from GaN to Ga-rich at the GaN sub-surface [1]. The Ga-rich phase can enhance the formation of Ti-Ga compound at the interface during the Ti deposition. The formation of Ti-Ga compound will increase the height and width of

the Schottky barrier. The formation of Ti-Ga compound will reduce the number of N-vacancies within the sub-surface of GaN, thus further increase the width of the Schottky barrier and reduce the electrical conductivity.

4.2 Effect of n-type GaN Crystal Orientation

Fig. 4.3 shows the DC *I-V* conduction profiles of as-deposited n-type GaN/Ti contacts formed on the (0001), $(000\bar{1})$, $(10\bar{1}0)$, and $(11\bar{2}0)$ surfaces of GaN. Two important features appear in the figure. One is that the profiles of all the contacts show a near-linear *I-V* relation, indicating that all contacts are ohmic in the as-deposited state. Therefore, the electrical conductance of each specimen is obtained as a single value from the gradient of each line. The *I-V* relation remains linear after annealing. The other feature

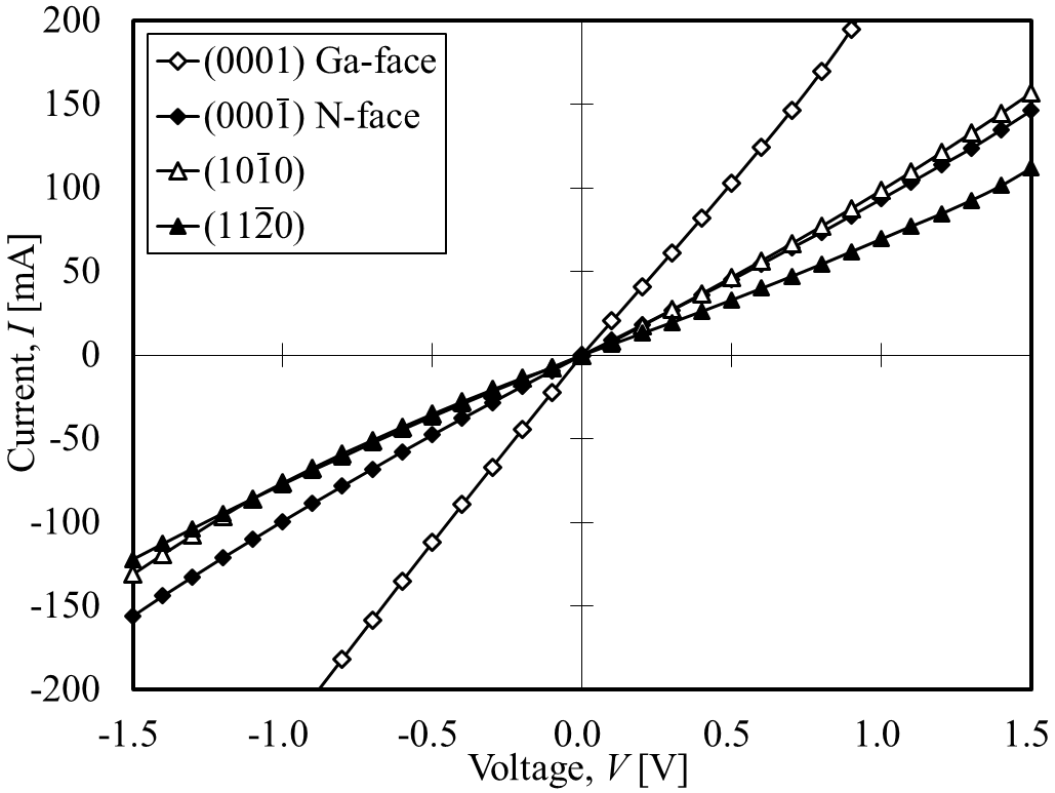

Fig. 4.3 *I-V* conduction profiles of as-deposited n-type GaN/Ti contacts formed on various surface of GaN [2].

is that the conductance changes depending on the surface orientation of GaN. The highest conductance is obtained with the contact on (0001). On the other hand, the conductance of the contacts formed on the other three surface orientations of GaN appears similar, as shown in the left part of Fig. 4.4.

Fig. 4.4 shows the changes in electrical conductance of the specimens depending on the annealing temperatures and time. In the annealing temperature of 773, 873 and 973 s, the holding time is set to zero. After reaching each designated temperature, the heater was switched off and the specimens cooled down by natural cooling. The heating rate and cooling rate are approximately 0.2 K/s and 0.7 K/s, respectively.

The change behavior of the contacts on (0001) appears different from that of the contacts on all other surface orientations. Although the highest conductance is obtained

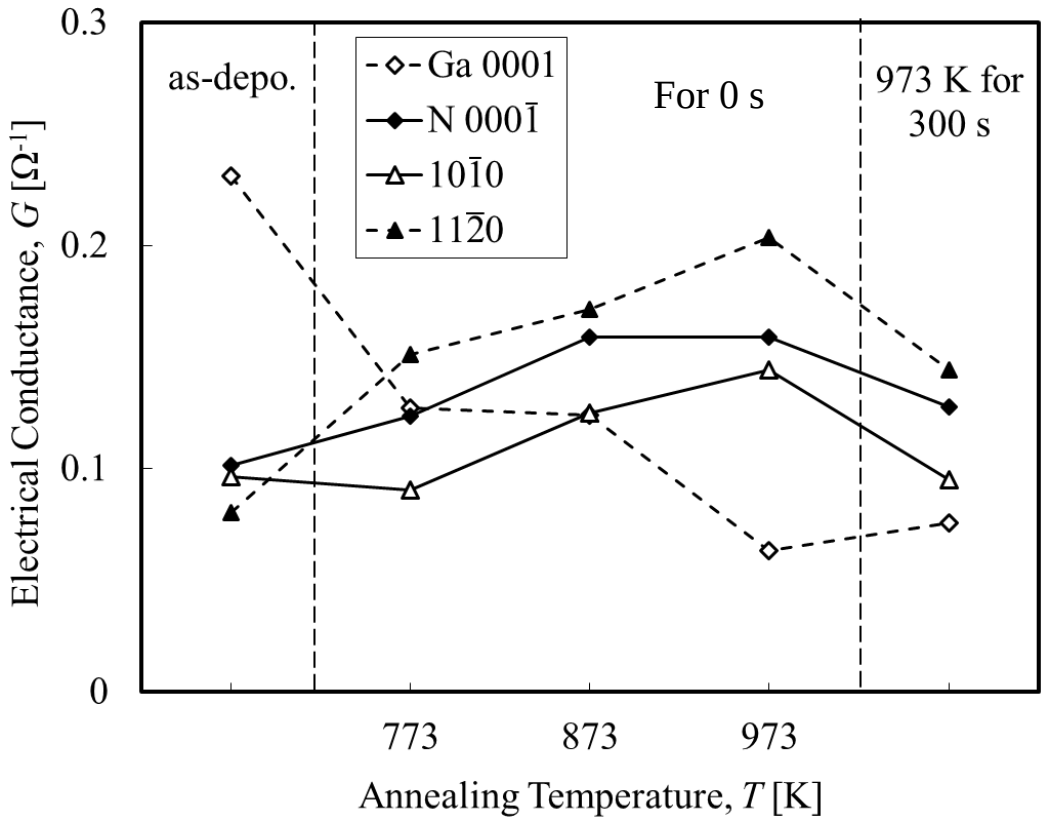

Fig. 4.4 Changes in electrical conductance (V =1.0 V) of the specimens depending on the annealing temperatures and times. The current were measured at 273 K [2].

with the contacts on (0001) in as-deposited state, the conductance deteriorates significantly by annealing even at a low temperature of 773 K for a very short time, and it becomes worse by annealing at higher temperatures. On the other hand, the conductance of the contacts on all other surface orientations of GaN is improved at first by annealing, and the improvement becomes larger by annealing at a higher temperature. However, the conductance of these specimens decreases upon extending the annealing time to 300 s at 973 K.

It is likely that the conductance is improved owing to the formation of N-vacancies in the GaN sub-interface by interfacial reaction between GaN and Ti [1]. On the other hand, the deterioration could be caused by excessive reactions that form byproduct phases such as Ti-Ga compounds. Thus, the deterioration of the conductance of the contacts is considered to be due to the transition from the interfacial reaction forming N-vacancies in GaN to that forming Ti-Ga compounds at the interface. The transition starts earlier and at a lower temperature in the contacts formed on (0001) than in those formed on other surface orientations.

Fig. 4.5 shows the XRD patterns of the contact specimens after annealing at 973 K for 300 s. In the patterns of the specimens formed on the (0001), $(10\bar{1}0)$, and $(11\bar{2}0)$ surfaces of GaN, peaks of GaN, Ti_2N, Ti_2Ga_3 and Ti_3Ga_5 are identified, whereas GaN and Ti appear in the pattern of the specimen formed on $(000\bar{1})$. Particularly, the peaks of Ti_3Ga_5 appearing in the pattern of the contact on (0001) are very strong, indicating that a considerable amount of Ti_3Ga_5 is formed at the interface. These results confirm the formation of Ti-Ga compounds at the interfaces with deteriorated electrical conductance. In addition, the reaction forming Ti-Ga compounds on the (0001) surface proceeds faster than that on the other surfaces of GaN.

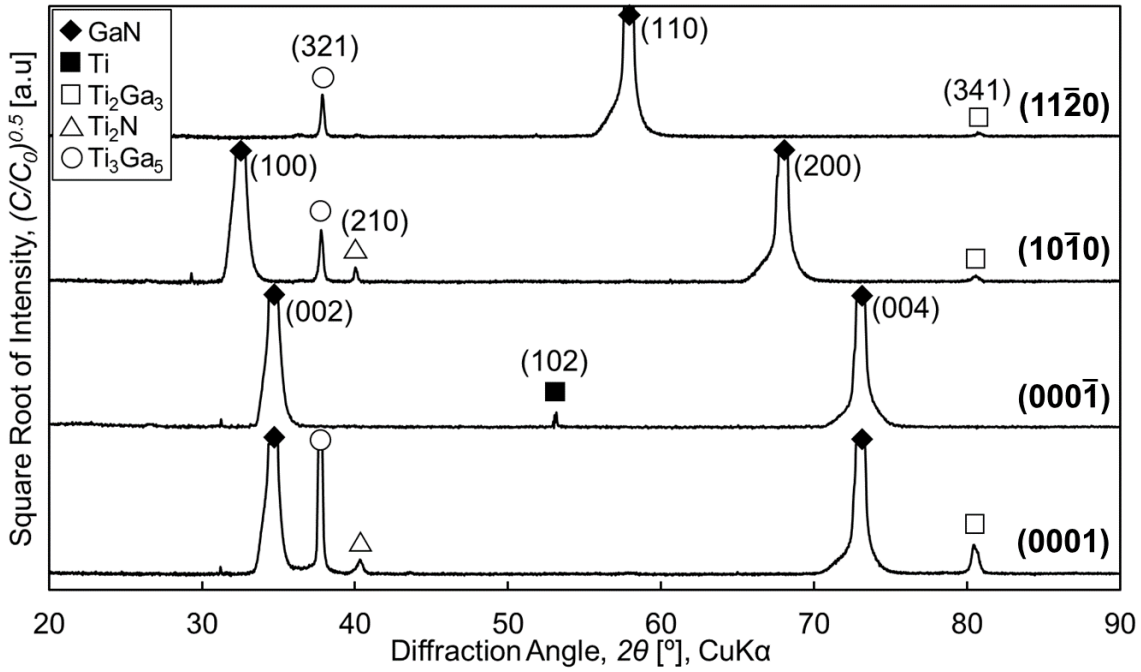

Fig. 4.5 XRD patterns of n-type GaN/Ti contacts formed on various surfaces of GaN after annealing at 973 K for 300 s: (0001), $(000\bar{1})$, $(10\bar{1}0)$ and $(11\bar{2}0)$ [2].

Fig. 4.6 shows an interfacial structure of n-type GaN/Ti contact formed on (0001) GaN surface after annealing at 973 K for 300 s. In the bright-field image shown in Fig. 4.6 (a), a 60-nm-thick layer is formed adjacent to GaN by the interfacial reaction. The layer has a polycrystalline structure which consists of equiaxed grains. The electron diffraction pattern corresponding to this area is shown in Fig. 4.6 (b) with some indices of diffraction spots. The patterns consists of a $[1\bar{2}10]$ zone axis net pattern of GaN [3] and randomly oriented spots from Ti_2Ga_3 [4] and Ti_3Ga_5 [5]. The dark-field image of the same area using the Ti_3Ga_5 (321) diffraction is shown in Fig 4.6 (c). Some grains in the layer adjacent to GaN appear bright, proving that the layer is Ti_3Ga_5. This result suggests that the interfacial reaction forming N-vacancies in GaN changes to that forming Ti-Ga compounds, i.e., from a donor-forming to a donor-eliminating reaction by excessive annealing. Therefore, to obtain a favorable ohmic interface, the interfacial reaction has to be controlled in order to prevent the formation of Ti-Ga compounds.

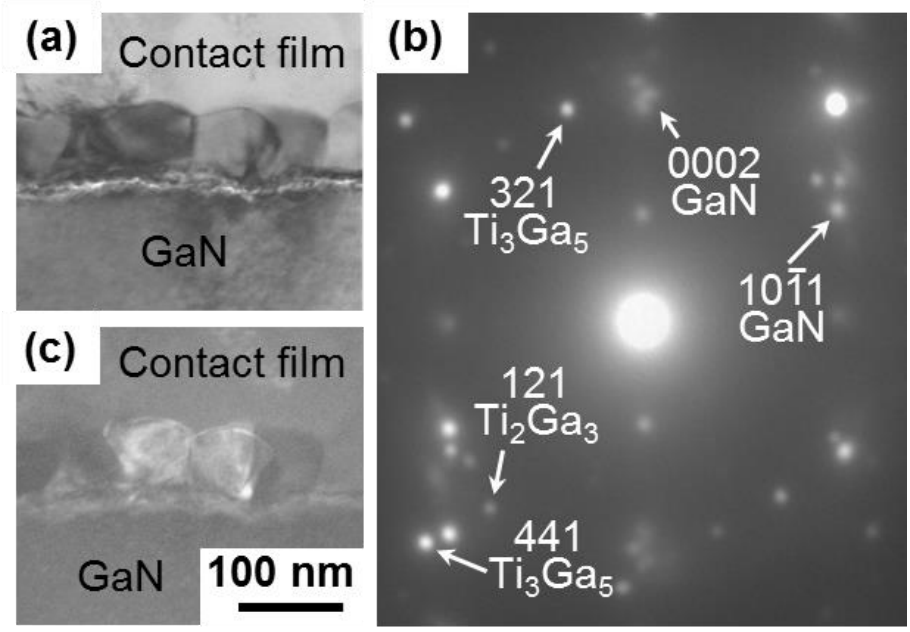

Fig. 4.6 Interfacial structure of n-type GaN/Ti contact formed on (0001) GaN surface after annealing at 973 K for 300 s. (a) bright-field image, (b) selected-area electron diffraction pattern corresponding to area shown in (a), (c) dark-field image of same area shown in (a) using Ti_3Ga_5 321 diffraction [2].

4.3 Summary

Ti contact films were formed on n-type GaN after Ar ion irradiation of the substrate for 300, 600, 1200, 2400 and 3600 s. Ti_2N is formed adjacent to substrate by the Ti deposition. It is likely that a huge amount of N-vacancies is formed within the GaN sub-surface near to the contact. *I-V* conduction profiles show that ohmic conduction is achieved. Furthermore, the conductance of the contacts is increased by prolonging the irradiation time. However, extensive irradiation more than 3600 s shows no further improvement in contact conductance. It is likely due to the phase transformation from GaN to Ga-rich at the GaN sub-surface. The Ga-rich phase enhanced the formation of Ti-Ga compound at the interface during the Ti deposition and reduce the number of N-vacancies within the sub-surface of GaN.

Ti contact films were formed on various orientation of GaN surface. The contact formed on (0001) Ga-face shows the highest electrical conduction in the as-deposited state. However, the conduction deteriorates by annealing even at a low temperature of 773 K. On the other hand, the conductance of the contacts on other three surfaces shows some improvement by annealing at 973 K. However the conductance deteriorates by further annealing at 973 K for 300s. The deterioration of the electrical conductance is attributed to the formation of Ti-Ga compound at the interface, as shown in the XRD patterns and TEM observation.

To improve the electrical conduction of n-type GaN contact, formation of sufficient N-vacancies within GaN sub-surface, adequate surface orientation of GaN and subsequent annealing condition has to be determined by considering the reaction occur between deposited film and GaN substrate.

Reference:

[1] A. b. M. Halil, K. Kimura, M. Maeda and Y. Takahashi, "Microstructures Observation of N-type GaN Contacts and the Electrical Properties", Transactions of JWRI 44, No. 1 (2015), 19-22.

[2] K. Kimura, A. b. M. Halil, M. Maeda and Y. Takahashi, "Effect of crystal orientation on ohmic contact formation for n-type gallium nitride," IOP Conference Series: Materials Science and Engineering 61 (2014), 012033 1-5.

[3] Powder Diffraction Files (Newtown Square, PA: ICDD) 50-792.

[4] Powder Diffraction Files (Newtown Square, PA: ICDD) 16-74.

[5] Powder Diffraction Files (Newtown Square, PA: ICDD) 42-811.

Chapter 5: Results and Discussion: p-type GaN: Contact Formation and Observation of Interfacial Structure

As discussed in Chapter 1 and 2, to form ohmic contact on p-type GaN, an appropriate contact material needs to be determined. For that purpose, to form Ti_3SiC_2, a Ti-Si-C ternary film with a composition stoichiometrically close to Ti_3SiC_2 has been deposited on p-type GaN. Ti_3SiC_2 is considered to improve the electrical conduction of the contact by work as a narrow-band gap intermediate semiconductor layer which reduces the Schottky barrier height at the interface [1, 2]. In this chapter, the interfacial structure of GaN/Ti-Si-C contact after annealed at 973 K and 1073 K (hold time were set to zero) will be discussed. The investigation of the interfacial structure of GaN and Ti_3SiC_2 are an important step to understand the practicality of this contact structure. Additionally, to improve the electrical conduction of p-type GaN contact by thinning the Schottky barrier at the interface, contact formation processes with a low annealing temperature have been investigated. For this purpose, the interfacial structures and electrical conductivities of conventional monolayer contacts of p-type GaN such as p-type GaN/Au and p-type GaN/Ni after annealing at lower temperatures (573 K and 673 K for 3600 s) will be examined and discussed.

5.1 p-type GaN/Ti-Si-C

It has been reported that p-type SiC/Ti/Al needs to be annealed up to 1273 K for 120 s or longer to form Ti_3SiC_2 phase on SiC [3]. In the present study, the Ti_3SiC_2 formation was carried out by annealing a Ti-Si-C ternary film with a composition stoichiometrically close to Ti_3SiC_2 at 973 K and 1073 K (hold time were set to zero). The

method applied in the present study has the advantages of lowering the annealing temperature and shortening the holding time. The lowering of the annealing temperature is achieved due to the fact that the deposited film is in a thermodynamically unstable state, resulting in the crystallization process that forms Ti_3SiC_2 phase being triggered at a lower temperature. However, the Ti_3SiC_2 formation by this method required a precise control of the deposited Ti-Si-C ternary film composition. In a p-type SiC study, it has been reported that TiC and $TiSi_2$ are formed instead of Ti_3SiC_2 by the annealing [4]. In the present study, a Ti-Si-C ternary film with a composition of 49 at.%Ti - 18 at.%Si - 33 at.%C have been formed on the substrate. This deposited film is stoichiometrically close to Ti_3SiC_2 (50 at.%Ti - 16.7 at.%Si - 33.3 at.%C).

However, due to the nature of p-type GaN that sensitive to high-temperature, there is a possibility that the annealing temperature of Ti_3SiC_2 formation applied in present study is too high. By annealing at high temperature, there is a possibility that the hole concentration of the p-type GaN is reduced and the dominant carrier-type is inverted. Nonetheless, to understand the practicality of this contact structure, it is an important and worthwhile to analyze and understand the interfacial structure of Ti_3SiC_2 on GaN substrates formed in the present study.

To investigate the dominant carrier-type of the specimens after the annealing at 973 K and 1073 K, the Hall-effect measurement has been performed at room temperature. The results revealed that the dominant carrier-type of both specimens were n-type, i.e., the dominant carrier-type of the specimens changed from p-type to n-type as a result of the annealing at 973 K and 1073 K. The factor that is likely to be the cause of this change is the increasing of N-vacancies in the p-type GaN sub-surface resulting from the out-diffusion of N atoms during the annealing. The formation of N-vacancies consequently

reduce the hole concentration of the p-type GaN. These vacancies are known to act as n-type dopant atoms with a donor level very close to the conduction band edge of n-type GaN [5].

From the Hall-effect measurement results, it can be understood that to form a contact between p-type GaN and Ti_3SiC_2, a contact formation with lower process temperature to form Ti_3SiC_2 is needed so that the dominant carrier type of the p-type GaN can be retained. For this purpose, an unconventional Ti_3SiC_2 formation method such as multilayer deposition by magnetron sputtering can be adopted [6]. It have been reported that by using three separate magnetrons with three element targets, Ti_3SiC_2 phase has been obtained at a deposition temperature of 923 K. Contact formation of Ti_3SiC_2 with low temperature such as this method can be referred and applied in the future study. However, it is likely that the interfacial structure of Ti_3SiC_2 formed in the present study and the one formed at lower temperature are identical to some extent.

To observe the interfacial structure of the formed Ti-Si-C contact on GaN after the annealing, XRD analysis and TEM observation have been performed. Fig. 5.1 shows the XRD patterns of the specimens in the as-deposited state and after the annealing at 973 K and 1073 K [7]. In the XRD pattern of the as-deposited specimen shown in Fig. 5.1 (a), a weak peak from Ti appears in addition to the strong peaks, which are identified as being from GaN and sapphire. Other than that, no peak related to Ti-Si-C phases was found. This analysis of as-deposited specimens indicates that the deposited film is in an amorphous state. The XRD pattern for the annealed specimens appear different than the patterns of the as-deposited specimen, as shown in Fig. 5.1 (b) and (c). Peaks corresponding to various crystallographic planes of Ti_3SiC_2 were identified. As a result

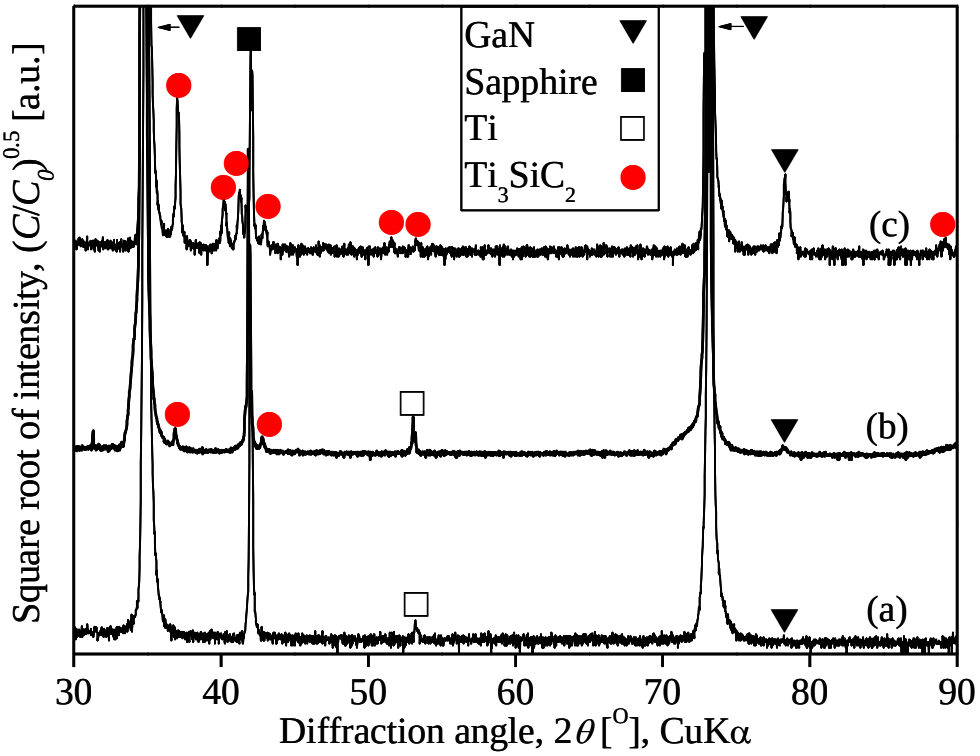

Fig. 5.1 XRD patterns of specimens. (a) As-deposited, (b) annealed at 973 K and (c) annealed at 1073 K [7].

of reducing the annealing temperature to 973 K from 1073 K, the residual Ti phase appeared, and fewer peaks corresponding to crystallographic planes of Ti_3SiC_2 were identified. The structural change of each of the two annealed specimens indicates that the Ti_3SiC_2 has a randomly oriented polycrystalline structure for each of the specimens. This proves that the Ti_3SiC_2 phase can be formed on GaN by deposition of the Ti-Si-C ternary film stoichiometrically close to Ti_3SiC_2 and subsequent annealing at 973 K or 1073 K.

In the present study, after reaching each designated temperatures (973 K or 1073 K), heater of the furnace was switched off and the specimens were cooled down by natural cooling, i.e., the holding time were set to zero. The heating rate and cooling rate are approximately 0.2 K/s and 0.7 K/s, respectively.

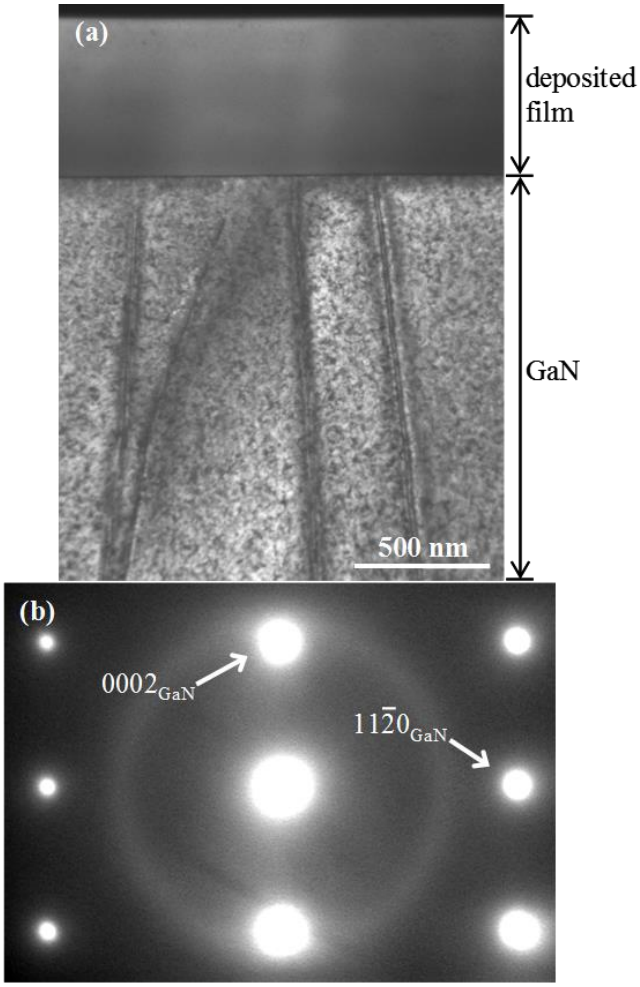

Fig. 5.2 Interfacial structure of as-deposited specimen. (a) bright-field image, (b) selected-area electron diffraction pattern corresponding to area shown in (a) [8].

The structure change during annealing has been analyzed further by TEM. Fig. 5.2 shows the structure of the as-deposited specimen [7]. Fig. 5.2 (a) shows a bright field image of the specimen. In the image, the deposited film of which thickness is approximately 500 nm appears in a monotonous contrast showing no grain boundaries within the film. Fig. 5.2 (b) shows the selected area electron diffraction pattern of the specimen. The diffraction pattern consists of $[1\bar{1}00]$ zone axis net pattern corresponding to GaN single crystal and a halo ring corresponding to amorphous phase. The results indicate that the deposited Ti-Si-C ternary film is in amorphous state, which agrees with

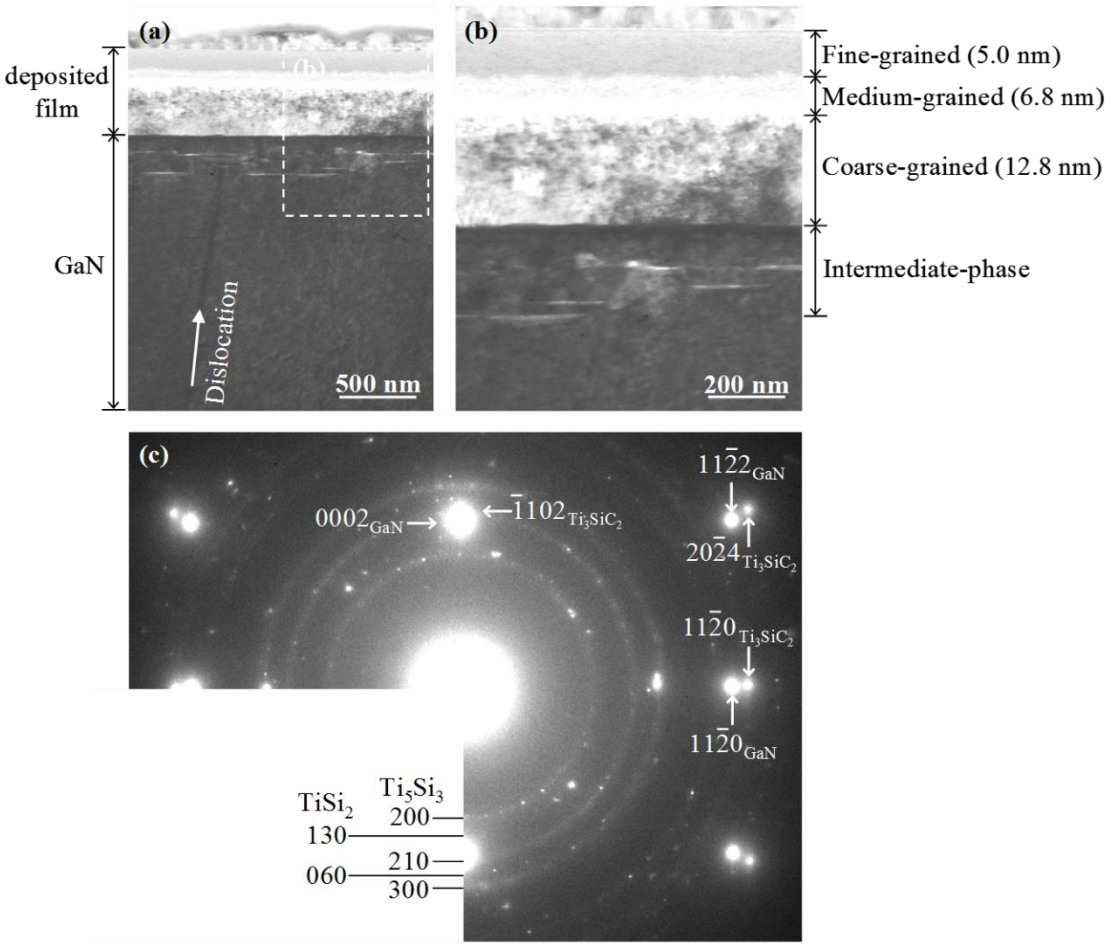

Fig. 5.3 Interfacial structure of specimen after annealing at 1073 K. (a) bright-field image, (b) high magnification bright-field image of area marked with dashed rectangle in (a), (c) selected-area electron diffraction pattern corresponding to area shown in (a) [8].

the XRD pattern shown in Fig. 5.1.

Fig. 5.3 shows the structure of the specimen after annealing at 1073 K [8]. In the bright-field image shown in Fig. 5.3 (a), the dislocation line of GaN stops near the contact interface between the GaN and deposited film, indicating that the GaN substrate near the contact interface have structurally transformed by annealing at 1073 K, forming a layer of intermediate-phase. The high magnification BFI shown in Fig. 5.3 (b) clearly shows that the single-layer Ti-Si-C ternary film of the as-deposited specimen has changed into three-layered film, distinct by the grain sizes. The grain sizes increase from coarse-

grained near the contact interface to fine-grained near the film surface, indicating that the structural change of the deposited film such as crystallization and nucleation start form the area near to the contact interface. Fig. 5.3 (c) shows the diffraction pattern corresponding to the area shown in Fig. 5.3 (a). This pattern consists of net patterns of GaN and Ti_3SiC_2 single crystals and Debye-Scherrer rings of Ti_5Si_3 and $TiSi_2$ polycrystals. The net pattern of GaN and Ti_3SiC_2 show a close correlation with each other as

$$(0002)\ \text{GaN}\ //\ (\bar{1}102)\ Ti_3SiC_2 \tag{5.1}$$

and

$$(11\bar{2}0)\ \text{GaN}\ //\ (11\bar{2}0)\ Ti_3SiC_2 \tag{5.2}$$

Therefore, it is considered that the Ti_3SiC_2 is formed adjacent to GaN epitaxially. On the other hand, the Debye-Scherrer rings of Ti_5Si_3 and $TiSi_2$ appear differently. The rings corresponding to Ti_5Si_3 are continuous, indicating that the grains of Ti_5Si_3 are very fine. The rings corresponding to $TiSi_2$ appear as discontinuous scattered spots, indicating that only a few grains of $TiSi_2$ are involved in the diffraction. Contrary with the analysis from XRD pattern, which shows that the film is consisting of polycrystals Ti_3SiC_2, the TEM observation shows that the selected area of the specimen shown in Fig. 5.3 (a) is consisting of single crystal Ti_3SiC_2. These observations reveal that most of the formed Ti_3SiC_2 in the film is polycrystalline Ti_3SiC_2. Single crystal Ti_3SiC_2 failed to be formed in most of the contact interface area likely due to the mismatch in lattice parameter between GaN and Ti_3SiC_2.

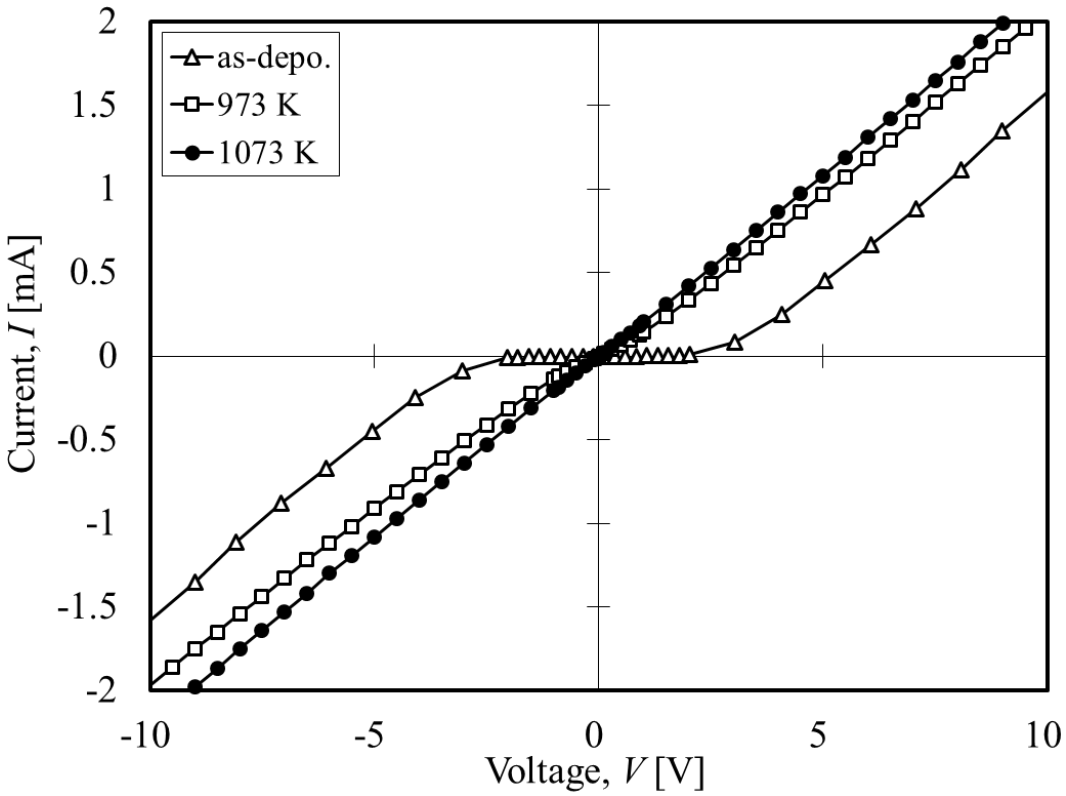

Fig. 5.4 *I-V* conduction profiles of specimens: as-deposited, annealed at 973 K and annealed at 1073 K [7].

Fig. 5.4 shows the changes in the electrical conduction profiles (*I-V* curves) caused by annealing the specimens at 973 K or 1073 K, where *I* is the current and *V* is the voltage between two adjacent electric pads [7]. The curve of the as-deposited specimen shows a non-linear relation between voltage and current, indicating that the formed contact is non-ohmic. On the other hand, near-linear relations between voltage and current are observed for both of the annealed specimens, indicating that ohmic-like contacts have been formed by the formation of Ti_3SiC_2 during annealing.

The Hall-effect measurement have revealed that the dominant carrier-type of both specimens in the present study are n-type, i.e., the dominant carrier-type of the specimens changes from p-type to n-type as a result of the annealing at 973 K and 1073 K. These results indicate that the observed non-ohmic contact of the as-deposited

specimen is formed between the p-type GaN and the deposited Ti-S-C ternary film. On the other hand, the observed ohmic-like contacts of the annealed specimens are formed between the n-type GaN (inverted from p-type GaN by annealing) and phases formed within the film during annealing. As shown in Fig. 5.3, other than the Ti_3SiC_2 phase, Ti_5Si_3 and $TiSi_2$ phases were also formed during the annealing. Due to the high work function of Ti_3SiC_2 (5.07 eV), it is most likely that the observed ohmic-like contacts of the annealed specimens are formed between the n-type GaN and these byproducts (Ti_5Si_3 and $TiSi_2$). The work functions of Ti_5Si_3 and $TiSi_2$, which are respectively 3.71 eV and 4.10 eV, are lower compared to that of Ti_3SiC_2. As discussed in Chapter 4, with formation of N-vacancies, ohmic contacts can be formed between n-type GaN and Ti even without annealing [9]. Thus, it is also possible that the observed ohmic-like contact of the annealed specimens is formed between n-type GaN and the residual Ti phase. Additionally, it also have been reported that n-type GaN ohmic contacts can also be achieved by the formation of the TiN phase through the reaction between GaN and Ti film during the annealing [5]. Although the TiN phase was not found in the XRD patterns in this study, there is a possibility that the observed ohmic-like contacts of the annealed specimens are between n-type GaN and TiN.

5.2 p-type GaN/Au

To investigate the dominant carrier-type of the specimens after the annealing at 573 K and 673 K for 3600 s, the Hall-effect measurement has been performed at room temperature. The results revealed that the dominant carrier-type of both specimens were p-type, i.e., the dominant carrier-type of the specimens could be retained after annealing at 573 K and 673 K 3600 s. These results suggest that no formation of N-vacancies in the p-type GaN sub-surface after the annealing processes. On the other hand, the Hall-effect measurement of the specimen annealed at 763 K revealed that the dominant carrier-type of the specimen was n-type, i.e., the dominant carrier-type of the specimen inverted from p-type to n-type as a result of the annealing at 773 K. This result suggests that by annealing p-type GaN at 773 K, N-vacancies have formed within the p-type GaN sub-surface. Hence, from these results, it can be concluded that annealing up to 673 K for 3600 s is appropriate to form p-type GaN/Au contact, while maintaining the p-type carrier.

To observe the interfacial structure of the formed Au contact on p-type GaN after the annealing, TEM observation and XRD analysis have been performed. Fig. 5.5 shows the interfacial structure of the p-type GaN/Au contact interface after annealing at 573 K for 3600 s [10]. As seen in the bright-field image shown in Fig. 5.5 (a), a layer of Au film with approximately 400-nm-thickness is observed adjacent to GaN substrate. The electron diffraction pattern of the whole area shown in Fig. 5.5 (a) was taken. The result is shown in Fig. 5.5 (b). The diffraction pattern consists of only net pattern of GaN. This result suggest that after the annealing at 573 K for 3600 s, the Au film is in a very early stage of crystallization. Thus, no diffraction pattern consisting of Au net pattern is observed.

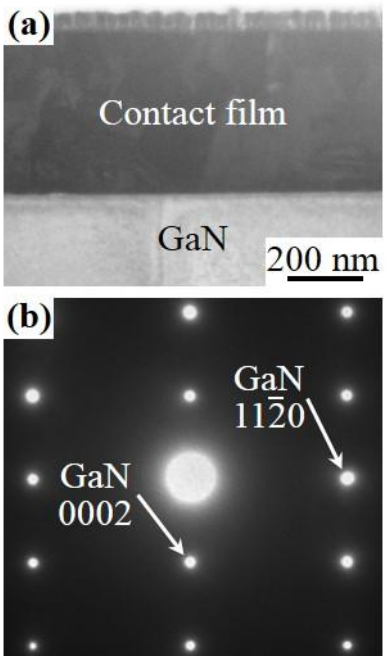

Fig. 5.5 Interfacial structure of p-type GaN/Au contact interface after annealing at 573 K for 3600 s. (a) bright-field image, (b) selected-area electron diffraction pattern corresponding to area shown in (a) [10].

Fig. 5.6 shows the XRD patterns of the p-type GaN/Au contact in the as-deposited state and after the annealing at 673 K for 3600 s. In the XRD pattern of the as-deposited specimen shown in Fig. 5.6 (a), strong peaks appear, which are identified as being from GaN and sapphire. Other than that, no peak related to Au phases was found. This analysis of as-deposited specimens indicates that the deposited film is in an amorphous state. The XRD pattern for the annealed specimens appear different than the patterns of the as-deposited specimen, as shown in Fig. 5.6 (b). Considerable strong peaks corresponding to crystallographic planes of Au were identified. These results indicate that after annealing 673 K for 3600 s stable phase of Au have been formed on the p-type GaN. The fact that the peak other than GaN, sapphire and Au is not observed indicates that no other compounds are formed, i.e. no reaction occurs at the interface between deposited Au film and GaN substrate during the annealing at 673 K. If the reaction occurs at the

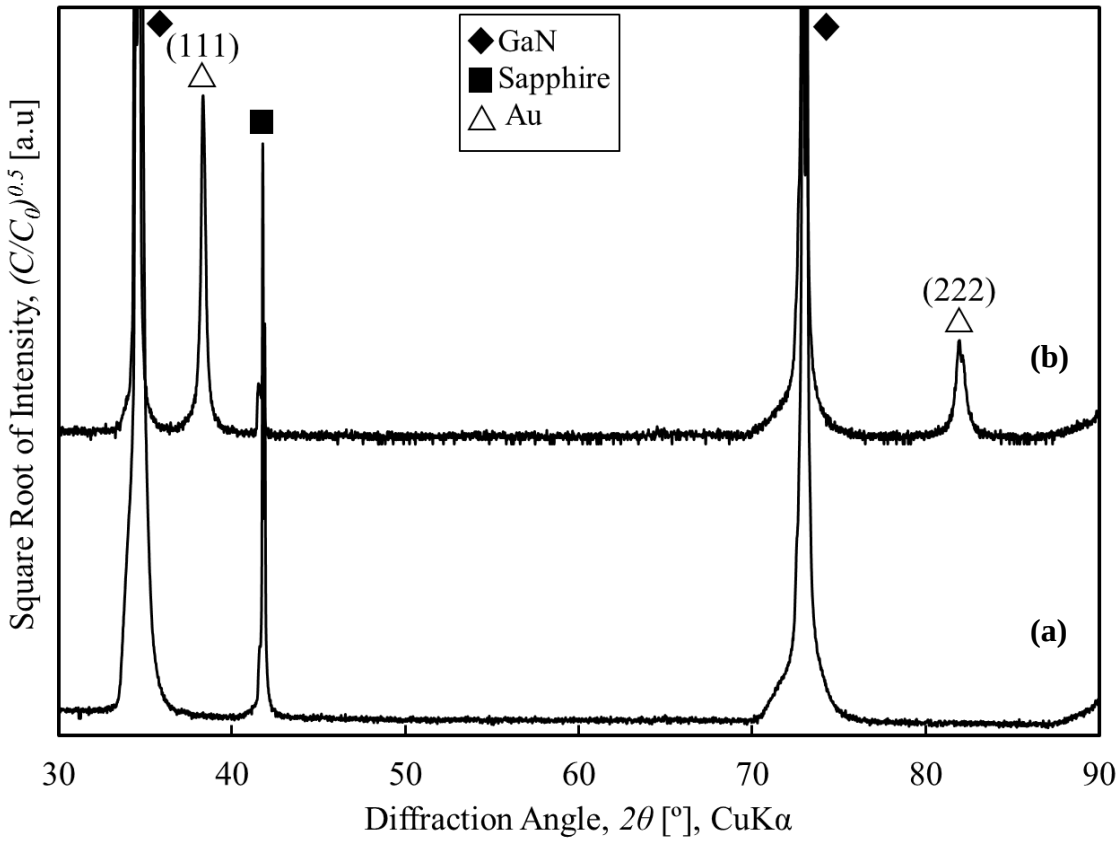

Fig. 5.6 XRD patterns of p-type GaN/Au contact interface after annealing at 673 K for 3600 s. (a) As-deposited, (b) annealed at 673 K for 3600 s.

interface between GaN and Au film, Au-Ga intermetallic compounds are expected to be produced at the interface.

Compared with Au, these intermetallic compounds have lower values of work functions. Thus, the formation of these compounds at the interface will increase the Schottky barrier (SB) height and deteriorate the electrical conduction of the contact. This reaction will also introduce unstable N atoms within p-type GaN substrates, which consequently diffuse to the interface of p-type GaN and Au film and form voids. The formation of voids at the interface decreases the area of contact interface and deteriorates the electrical conduction of the p-type GaN/Au contact. Hence, by annealing the p-type GaN/Au contact at 573 K and 673 K for 3600, the deterioration of electrical conduction

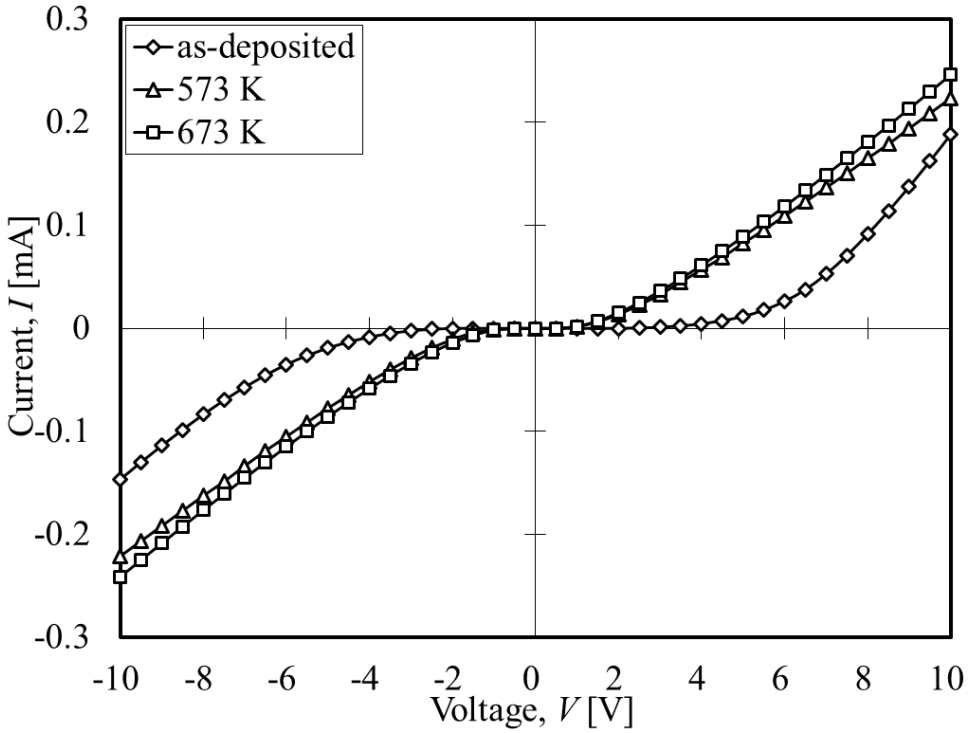

Fig. 5.7 *I-V* conduction profiles of p-type GaN/ Au contacts: as-deposited, annealed at 573 K for 3600 s and annealed at 673 K for 3600 s.

of the contact have been avoided.

Fig. 5.7 shows the electrical conduction profile (*I-V* curves) of the samples, where *I* is the current and *V* is the voltage between two adjacent electric pads. The curve of the as-deposited and annealed specimens show a non-linear relation between voltage and current, indicating that the formed contacts is non-ohmic. However, the electrical conduction profiles of the specimens annealed at 573 K and 673 K for 3600 s show some improvement compared to the electrical conduction profile of the as-deposited specimens.

Due to no dominant carrier-type and structural changes during the annealing as shown by the Hall-effect measurement, TEM and XRD observations, this electrical conduction improvement can be attribute to the enhancement of hydrogen (H) release from p-type GaN by the annealing at 573 K and 673 K for 3600 s. The carrier (accepter) concentration is increased by the H release and consequently reduce the SB width at the

contact interface. As a result, electrical conduction of the contacts are improved.

During the growth process of GaN, H is dissolved into GaN exceeding the saturated point due to the very high concentration of H in the process ambient. H formed neutral Mg-H complexes within p-type GaN, thus cannot be released without annealing. Therefore, the postgrowth activation of Mg by annealing at 973 K, which releases H from GaN is necessary. However, residual H still presence within p-type GaN even after the postgrowth annealing process. The H release by annealing at 573 K and 673 K for 3600 s in present study indicates most of the H incorporated during growth process of GaN still exists even after the postgrowth annealing process at 973 K. The H within p-type GaN must be still in supersaturated state because H must still combine with Mg, thus can be released by annealing even at low temperatures (573 K and 673 K for).

As shown by the results of p-type GaN/Ti-Si-C contacts after the annealing, a higher temperatures of contact formation (973 K and 1073 K) are proven not suitable for the H release. This due to the increasing of N-vacancies in the p-type GaN sub-surface resulting from the out-diffusion of N atoms during the annealing at high temperature. The formation of N-vacancies consequently reduce the hole concentration of the p-type GaN and consequently inverted the dominant carrier-type of the substrate.

5.3 p-type GaN/Ni

The same procedure performed to p-type GaN/Au specimens is carried out on the p-type GaN/Ni specimens. To investigate the dominant carrier-type of the specimens after the annealing at 673 K for 3600 s, the Hall-effect measurement has been performed at room temperature. The results revealed that the dominant carrier-type of the specimen was p-type i.e., the dominant carrier-type of the specimen could be retained after annealing at 673 K 3600 s. These results suggest that no formation of N-vacancies in the p-type GaN sub-surface after the annealing processes. On the other hand, the Hall-effect measurement of the specimen annealed at 763 K revealed that the dominant carrier-type of the specimen was n-type, i.e., the dominant carrier-type of the specimen inverted from p-type to n-type as a result of the annealing at 773 K. This result suggests that by annealing p-type GaN at 773 K, N-vacancies have formed within the p-type GaN sub-surface. Hence, from these results, it can be concluded that annealing up to 673 K for 3600 s is appropriate to form p-type GaN/Ni contact, while maintaining the p-type carrier.

To observe the interfacial structure of the formed Ni contact on p-type GaN after the annealing, TEM observation has been performed. Fig. 5.8 shows the interfacial structure of the p-type GaN/Ni contact interface after annealing at 673 K for 3600 s. As seen in the bright-field image shown in Fig. 5.8 (a), a layer of Au film with approximately 350-nm-thickness is observed adjacent to GaN substrate. The electron diffraction pattern of the whole area shown in Fig. 5.8 (a) was taken. The result is shown in Fig. 5.8 (b). This pattern consists of net patterns of GaN single crystals and Debye-Scherrer rings of Ni polycrystals. The rings corresponding to Ni are continuous, indicating that Ni polycrystalline with small grains size are formed within the contact after annealing.

Identical to the observation on the p-type GaN/Au contact interface after

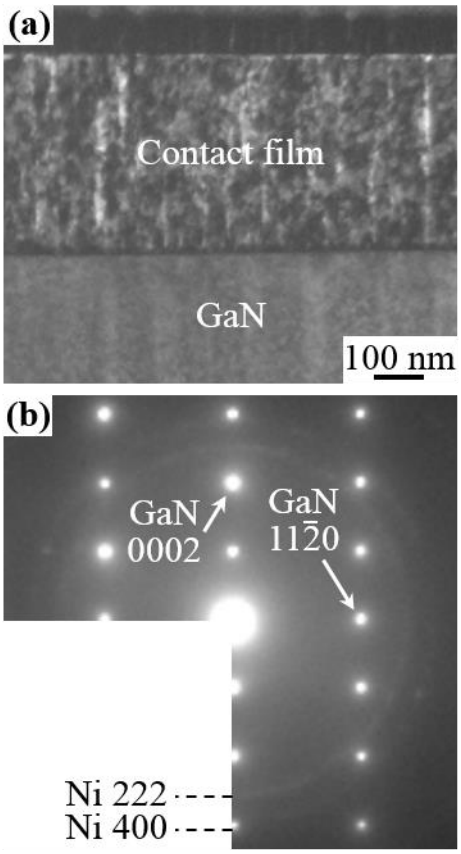

Fig. 5.8 Interfacial structure of p-type GaN/Ni contact interface after annealing at 673 K for 3600 s. (a) bright-field image, (b) selected-area electron diffraction pattern corresponding to area shown in (a).

annealing, these results indicate that no reaction occurs at the interface between deposited Ni film and GaN substrate during the annealing at 673 K for 3600. If some reaction occurs at the interface between GaN and Ni film, Ni-Ga intermetallic compounds will be formed at the interface. Compared with Ni, these intermetallic compounds have lower values of work functions. Thus, the formation of these compounds at the interface will increase the SB height and deteriorate the electrical conduction of the contact. This reaction will also introduce unstable N atoms within p-GaN substrates, which consequently diffuse to the interface of p-GaN and Ni film and form voids. The formation of voids at the interface decreases the area of contact interface and deteriorates the electrical conduction of the p-

GaN/Ni contact. As seen in Fig. 5.8 (a), no reaction layers and void form at the interface. So, the reaction of Ni-Ga under the annealing condition of 573 K for 3600 s can be negligible, i.e., the deterioration of electrical conduction of the contact have been avoided by annealing at low temperature.

Fig. 5.9 shows the electrical conduction profile (*I*-*V* curves) of the samples, where *I* is the current and *V* is the voltage between two adjacent electric pads [11]. The curve of the as-deposited and annealed specimens show a non-linear relation between voltage and current, indicating that the formed contacts is non-ohmic. However, identical to the electrical conduction of p-type GaN/Au contacts after annealing, the electrical conduction profiles of the p-type GaN/Ni contacts annealed at 573 K and 673 K for 3600 s show some improvement compared to the electrical conduction profile of the as-deposited specimens.

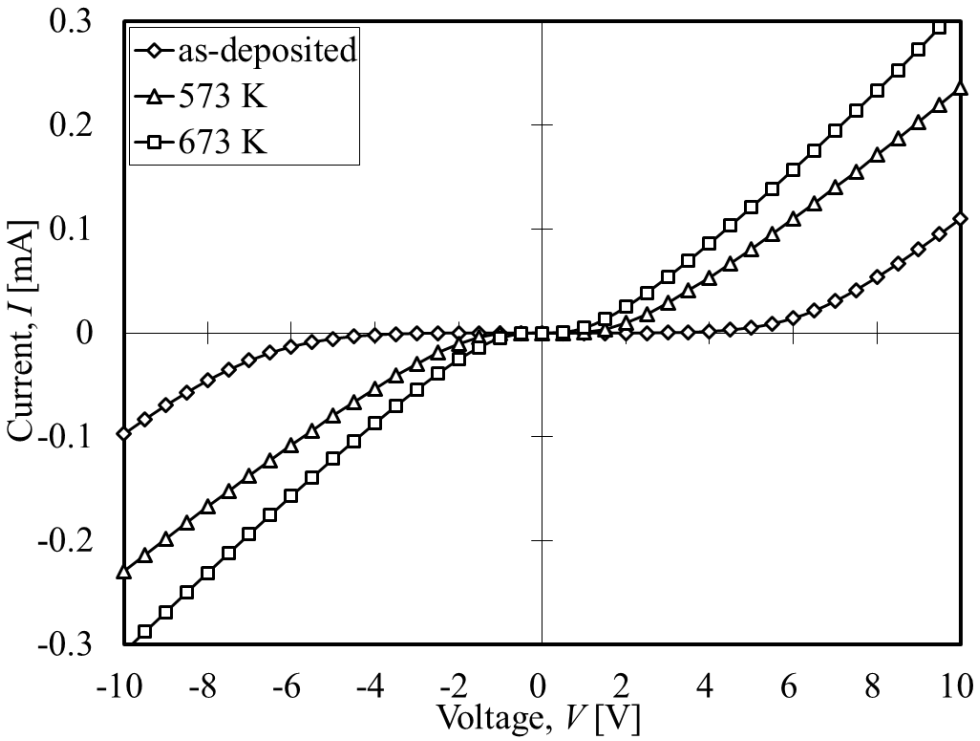

Fig. 5.9 *I*-*V* conduction profiles of p-type GaN/ Ni contacts: as-deposited, annealed at 573 K for 3600 s and annealed at 673 K for 3600 s [11].

As shown by the Hall-effect measurement and TEM observations, no dominant carrier-type and structural changes occur after the annealing. Therefore, the improvement of electrical conduction of the contacts can be attribute to the enhancement of H release from p-type GaN by the annealing at 573 K and 673 K for 3600 s. The carrier concentration is increased by the H release and consequently reduce the SB width at the contact interface. As a result, electrical conduction of the contacts are improved. These results agree with the result obtained by annealing p-type GaN/Au contacts. H within p-type GaN can be released by annealing even at low temperatures (673 K for 3600 s). Therefore, it can be conclude that annealing at 673 K for 3600 s is an adequate annealing condition to form Au and Ni contacts on p-type GaN, while improving the electrical conduction and maintaining the p-type carrier.

5.4 Summary

In this chapter, to the investigation of the interfacial structure of GaN and Ti_3SiC_2, Ti-Si-C ternary film with a composition stoichiometrically close to Ti_3SiC_2 has been deposited on p-type GaN. Polycrystalline Ti_3SiC_2 phase has been formed on the substrate after annealing at 973 K and 1073 K. However, after the annealing at 973 K and 1073 K, the dominant carrier-type of p-type GaN has inverted to n-type. This is likely due to the increasing of N-vacancies in the p-type GaN sub-surface resulting from the out-diffusion of N atoms during the annealing at high temperature. The direct-current conduction test shows that ohmic-like contacts have been achieved after the annealing. These ohmic-like contacts are likely formed between n-type GaN (inverted from p-type by the annealing) and the byproducts of Ti_3SiC_2 formation (Ti_5Si_3 and $TiSi_2$), the residual Ti phase and/or the TiN phase.

The investigation of the interfacial structure and electrical conduction of p-type GaN/Au and p-type GaN/Ni contacts after annealing at 673 K for 3600 s show some identical results. The dominant carrier-type of both contacts are maintained after the annealing. XRD analysis and TEM observation of both contacts revealed that the no intermetallic compound is formed at the interface after the annealing. Furthermore, the electrical conduction profile of these contacts show some improvement after the annealing at 573 K and 673 K for 3600 s. From these investigations, it can be conclude that annealing at 673 K for 3600 s is an adequate annealing condition to form Au and Ni contact on p-type GaN, while improving the electrical conduction and while maintaining the p-type carrier.

References:

[1] B J Johnson and M A Capano, "Mechanism of ohmic behavior of Al/Ti contacts to p-type 4H-SiC after annealing," Journal of Applied Physics 95 (2004), 5616-5620.

[2] S Tsukimoto, K Nitta, T Sakai, M Moriyama and M Murakami, "Correlation between the electrical properties and the interfacial microstructures of TiAl-based ohmic contacts to p-type 4H-SiC," Journal of Electronic Materials 33 (2004), 460-466

[3] M. Maeda and Y. Takahashi, "Control of interfacial properties in power electronic devices," International Journal of Nanotechnology 10 (2013), 89-99.

[4] K. Takahashi, M. Maeda, N. Matsumoto and Y. Takahashi, "Formation of Ti_3SiC_2 Contact Layer Preventing Interfacial Reaction with SiC Substrate," 14^{th} Symposium on Microjoining and Assembly Technology in Electronics (Mate

2008) 14 (2008), 343-346.

[5] S. N. Mohammad, “Contact mechanisms and design principles for alloyed ohmic contacts to n-GaN,” Journal of Applied Physics 95 (2004), 7940-7953.

[6] V. Vishnyakov, J Lu, P Eklund, L Hultman and J Colligon, “Ti_3SiC_2-formation during Ti-C-Si multilayer deposition by magnetron sputtering at 650 C,” Vacuum 93 (2013), 56-59.

[7] A. b. M. Halil, M. Maeda and Y. Takahashi, “Effect of Ti_3SiC_2 formation on p-type GaN by vacuum annealing on the contact properties,” IOP Conference Series: Materials Science and Engineering 61 (2014) 012034.

[8] A. b. M. Halil, M. Maeda and Y. Takahashi, “Interfacial Nanostructure and Electrical Properties of Ti_3SiC_2 Contact on p-Type Gallium Nitride,” Materials Transactions 54, No. 6 (2013) 890-894.

[9] M. Maeda, T. Yamasaki and Y. Takahashi, “Ohmic Contact Mechanism of Titanium-based electrodes on n-type Gallium Nitride,” Transactions of JWRI 41 No. 1 (2012), 45-48.

[10] A. b. M. Halil, K. Tsuchida, M. Maeda and Y. Takahashi, “Improvement of Electrical Properties of p-type GaN and Au Contact Interface,” Quarterly Journal of the Japan Welding Society 33, No. 2 (2015) 84s-87s.

[11] A. b. M. Halil, K. Tsuchida, M. Maeda and Y. Takahashi, “Ni Nano Level Thin Film Formation on p-GaN and Improvement of Electrical Properties by Hydrogen Release Enhancement,” Journal of Smart Processing 4, No. 2 (2015) 109-114.

Chapter 6: Results and Discussion: p-type GaN: Hydrogen Release Enhancement by Applying Current Flow during Annealing

In the previous chapter, it has been discussed that to improve the electrical conduction and while maintaining the p-type carrier of p-type GaN contact, annealing process with low annealing temperature (673 K) is necessary. In this chapter, in order to further improve the electrical conduction of Mg-doped p-type GaN contacts, enhancement of hydrogen release from GaN substrates is attempted. During substrate growth process, hydrogen is incorporated into the substrates [1]. The presence of hydrogen within Mg-doped p-type GaN substrates passivates the acceptors within GaN by forming a neutral Mg-H complex, lower the carrier concentration and subsequently deteriorate the electrical conduction of p-type GaN contacts [2-5]. To release hydrogen from GaN substrate, annealing at high temperature is necessary [6]. In this chapter, a new method to release hydrogen from GaN substrates at lower temperature is proposed [7]. By applying current flow through the GaN substrates during annealing process, hydrogen within GaN substrates can be released even at low temperature. To understand the mechanism of hydrogen release by applying current flow during annealing, the change in current values p-type GaN contacts during annealing are observed and analyzed.

6.1 Improvement of Electrical Conduction by Applying Current Flow during Annealing

Fig. 6.1 shows the electrical conduction profiles (*I*-*V* curves) of the p-type GaN/Ni contacts (as-deposited, annealed at 573 K and 673 K for 3600 s, annealed at 573 K and 673 K for 3600 s while applying current flow under condition of 30 V), where *I* is

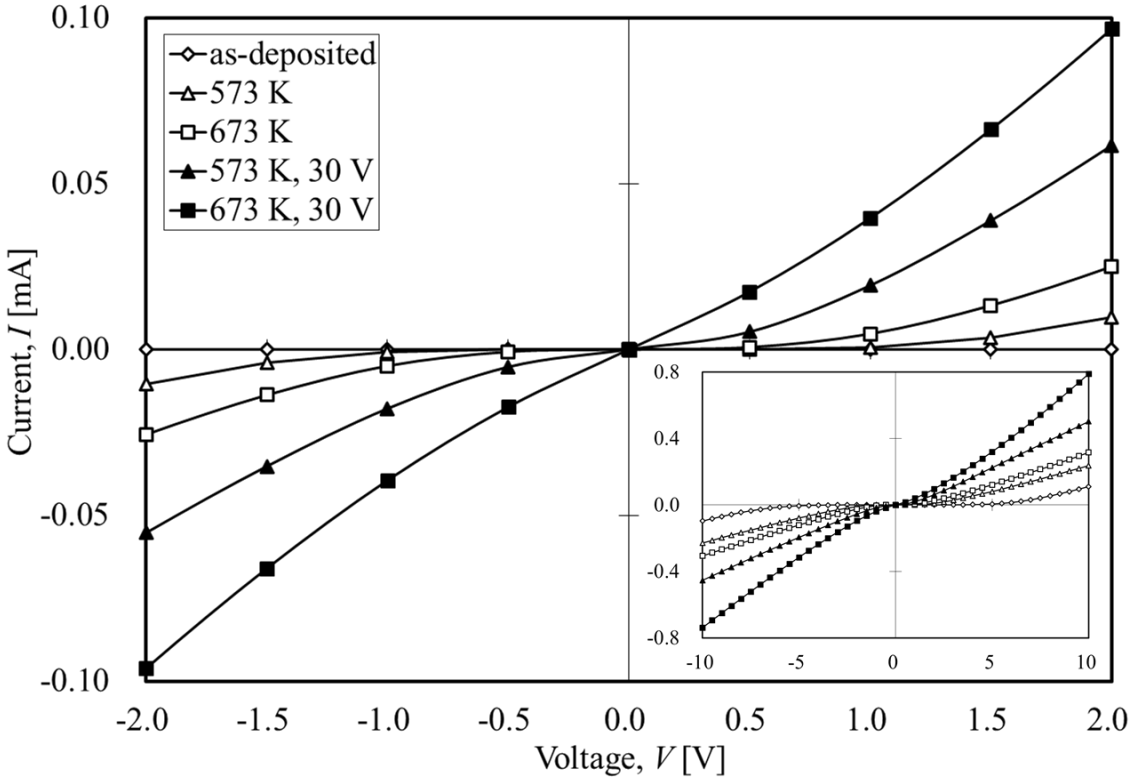

Fig. 6.1 *I-V* conduction profiles of p-type GaN/Ni contacts: as-deposited, annealed at 573 K and 673 K for 3600 s, annealed at 573 K and 673 K for 3600 s while applying current flow under condition of 30 V.

the current and *V* is the voltage between two adjacent electric pads. The electrical conduction profiles of the specimens annealed at 573 K and 673 K for 3600 s without current flow (marks of △ and □) show some improvement compared to the electrical conduction profile of the as-deposited specimen (marks of ◇).

During the growth process of Mg-doped p-type GaN, the ambient of hydrogen (H) with high partial pressure is involved. Hence, the concentration of H incorporated within GaN during the growth process is higher than the saturation point of H in GaN, resulting in supersaturated state of H within GaN. As discussed in the previous chapter (p-type GaN/Au and p-type GaN/Ni contacts), after the annealing process, no changes in dominant carrier-type and contact structure occur. Thus, the improvement of electrical conduction can be attribute to the H release from p-type GaN by the annealing at 573 K

and 673 K. The carrier (accepter) concentration is increased by the H release and consequently reduce the Schottky barrier (SB) width at the contact interface. As a result, electrical conduction of the contacts are improved even under low temperature annealing condition. However, amount of H released by this method is dependent to the H concentration within p-type GaN and the annealing temperature. At a constant temperature, when the H concentration within p-type GaN decrease and reach a saturation point of H in GaN, no more H is released. This saturation point must still be much higher than the equilibrium solubility of H in GaN.

By applying current flow through the substrates during annealing at 573 K and 673 K for 3600 s (marks of ▲ and ■), some further improvements of electrical conduction are achieved, notably at low values of voltage, as can be seen in Fig. 6.1. These further improvements of electrical conduction of the contacts imply that significant amount of H within p-type GaN has been released by applying current flow during annealing at 573 K and 673 K. The amount of H released from p-type GaN subjected to current flow during annealing must be much higher compared to without the current flow.

6.2 Kinetic Model of the Hydrogen Release Mechanisms by Applying Current Flow during Annealing

To understand the mechanisms of H release from p-type GaN by applying current flow during annealing, the change in current values of p-type GaN contacts during annealing has been observed. Multiple mechanisms that work in parallel with each other are corresponding to this H release. It is initially assumed that they work independently to each other, although there remains a possibly that they sometimes work dependently. The mechanisms of H release can be understand by analyzing the change in current values

of the contacts during the annealing based on a kinetic model. In the kinetic model, it is assumed that the mechanisms are independent to each other. Then, the change in current values of the contacts can be expressed by the following equation.

Normalize values of current $(\Delta I/I_0)$ is given by

$$(\Delta I/I_0) = \left(\frac{I - I_0}{I_0}\right) = \sum_{k=1}^{n} a_k \left(1 - exp\left(-\frac{t}{\tau_k}\right)\right), \quad (6.1)$$

where, a represents the saturation value and τ represents the exponential decay with time constant of the relevance mechanisms of H release. The integer k (numbers of the term in the kinetic model), corresponds to the number of the H release mechanisms during the annealing. For example, first mechanism of H release: k = 1, second mechanism of H release: k = 2 and so on. Additionally, the number of H release mechanisms are correlate to the annealing condition and contact structure.

Theoretically, it is possible to express one mechanism of H release by using more than one term in the model, i.e., integer k is larger than the number of the H release mechanisms. However, in this case, it is difficult to distinguish the corresponding mechanism for each terms in the model. Thus, it is best to express each mechanism of H release by using single term in the model.

In the present study, the change in current values of three different annealing and contact conditions has been observed; (a) annealing p-type GaN/Ni contact at 673 K without current flow, (b) annealing p-type GaN/Ni contact at 673 K while applying current flow under the condition of 10 V and (c) annealing p-type GaN/Pd contact at 673 K while applying current flow under the condition of 10 V. To express the change of current values of these three cases with the kinetic model, the number of corresponding

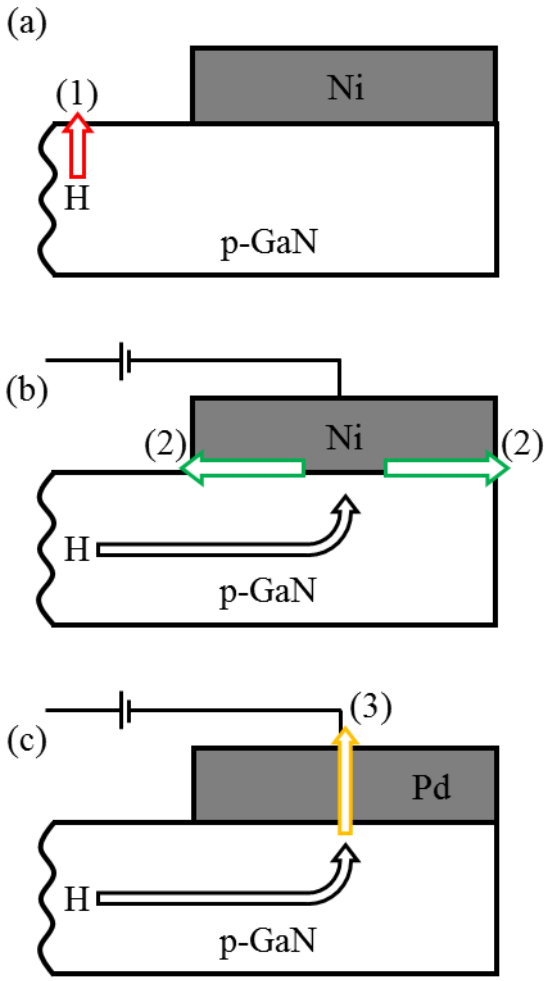

Fig. 6.2 Schematic illustrations of the H release mechanisms from p-type GaN substrate; (a) H release through the exposed surface by thermal annealing, (b) H release through the contact interface by applying current flow during annealing (c) H release through Pd film by applying current flow during annealing.

H release mechanism for each case (model) need to be determined.

Fig. 6.2 shows the schematic illustrations of the H release mechanisms from p-type GaN substrate. The illustrated arrows indicate the H release mechanisms. In the case of annealing p-type GaN/Ni contact at 673 K without applying current flow, the corresponding H release mechanism is H release through the exposed surface by thermal annealing, as illustrated by red arrow in Fig. 6.1 (a). In this case, the H release is only occurs by one mechanism, i.e., k = 1. By increasing the temperature of the substrates

during annealing, the bond of neutral Mg-H complexes within p-type GaN brake and H can be released from GaN substrate. The mechanism of this H release is driven by the supersaturated state of H within GaN. The reactions that related to this mechanism of H release are show by the following equations.

Dissociation of Mg-H complex occurring within GaN;

$$Mg\text{-}H \rightarrow Mg^{-} + H^{+}. \quad (6.2)$$

Desorption of H gas from the exposed surface;

$$2H^{+} \rightarrow H_2\ (gas). \quad (6.3)$$

It has been reported that the Mg-H complex dissociation process can occur even at low temperature. Additionally, based on a density-functional theory, the obtained diffusion activation energy of H ion indicate that H ion within GaN have high mobility [8]. Thus, it can be expected that the dissociation of Mg-H complex (Eq. 6.2) and H movement to the GaN surface are not the rate-determining step of this H release process. Instead, desorption of H gas from GaN surface (Eq. 6.3) is expected to be the rate-determining step of this H release process.

The electrical conduction improvement by H release of this mechanism can be observe in the results of annealing p-type GaN/Ni contacts at 673 K for 3600 s, as shown in Fig. 6.1. However, as discussed above, the amount of H released by this mechanism is dependent to the H concentration within p-type GaN and the annealing temperature. Under a constant temperature, when the H concentration within p-type GaN decreases and reach a saturation point of H in GaN at 673 K, no more H is released. This saturation

point must still be much higher than the equilibrium solubility of H in GaN.

The change in current values corresponding to the H release in this model can be expressed by the following equation.

$$(\Delta I/I_0)_{Ni(annealing)} = a_{1,1}\left(1 - exp\left(-\frac{t}{\tau_{1,1}}\right)\right) \quad (6.4)$$

In the case of annealing p-type GaN/Ni contact at 673 K while applying current flow of 10 V, the corresponding mechanisms of H release are H release through the exposed surface by thermal annealing (red arrow in Fig. 6.1 (a)) and H release through the contact interface by applying current flow during annealing (green arrow in Fig. 6.1 (b)). In this case, the H release is occurs by two mechanisms, i.e., $k = 2$. In the early stage of annealing, the same mechanism as in the previous model is dominant, i.e., H released through exposed p-type GaN surface by the thermal annealing (red arrow in Fig. 6.1 (a)).

At the same time, by increasing the temperature of the substrates during annealing, the bond of neutral Mg-H complexes within p-type GaN brake, and H gain enough mobility to be effected by the current flow. H is moved near the interface between p-type GaN and Ni contact by the applied current flow, as shown as black arrow in Fig. 6.1 (b). However by moving H near the interface by applying current flow, the H concentration of other area of p-type GaN decreases. Thus, the H released through exposed p-type GaN surface by thermal annealing is reduced (red arrow in Fig. 6.1 (a)). After H is moved near to the interface between p-type GaN and Ni film contact by applied current flow during annealing, H diffuse along the interface to the expose surface and released from GaN substrate. H cannot be diffuse and released through Ni contact because H is not soluble in Ni at all. In the later stage of the annealing, this mechanism of H release

is dominant. This mechanism is illustrated by green arrow mark as (2) in Fig. 6.1 (b). At this stage, it is unknown whether the formation of H gas (Eq. 6.3) occur when H reach at the contact interface (black arrow → formation of H gas → green arrow) or when H reach at the exposed surface (black arrow → green arrow → desorption of H gas at the surface). However, it is not known which step is the rate-determining step of this process. As discussed above, H within GaN have high mobility. Furthermore, the H mobility will further enhance by applying the current flow. Thus, H movement to the contact interface between p-type GaN and Ni contact (black arrow) is not the rate-determining step of this H release process. Therefore, the rate-determining step of this H release process can be either the formation of H gas at the contact interface, the diffusion of H gas along the contact interface or the desorption of H gas from GaN surface.

Nevertheless, the applied current flow will create a constantly high concentration of H in the area close to the interface (cathode). H release by this mechanism will keep occurring until the H concentration in the area close to the interface is reduced and reach a saturation point of H in GaN at 673 K, Thus, the driven mechanism of H release is thermal annealing and the high local concentration of H near the contact interface induced by the applied current flow. The change in current values corresponding to the H release in this model can be expressed by the following equation.

$$(\Delta I/I_0)_{Ni(annealing+current\ flow)} = a_{2,1}\left(1 - exp\left(-\frac{t}{\tau_{2,1}}\right)\right) + a_{2,2}\left(1 - exp\left(-\frac{t}{\tau_{2,2}}\right)\right) \quad (6.5)$$

In the case of annealing p-type GaN/Pd contact at 673 K while applying current flow of 10 V, there are three corresponding mechanisms of H release, i.e., k = 3. During the annealing, the same two mechanisms as in the two previous model are dominant, i.e., H release through the exposed surface by thermal annealing (red arrow in Fig. 6.1 (a)) and H release through the contact interface by applying current flow during annealing (green arrow in Fig. 6.1 (b)). However, in addition to these mechanism, H also released from GaN substrate by diffuse through Pd contact, as shown as yellow arrow marked in Fig. 6.1 (c). This H release mechanism is also driven by the thermal annealing and high local concentration of H near the contact interface induced by the applied current flow. However, instead of diffuse along the contact interface, H diffuse through the Pd contact and release from the Pd surface. Therefore, this mechanism of H release also driven by the and by the fact that H is soluble in Pd [9-10]. Due to the comparably high mobility of H in GaN [8] and Pd [10], it is expected that desorption of H gas at the Pd surface (Eq. 6.3) to be the rate-determining step of this process.

All of these mechanisms of H release occur in parallel during the annealing. However, based on the stage of the annealing, some mechanisms will become dominance compared to others. The change in current values corresponding to the H release in this model can be expressed by the following equation.

$$(\Delta I/I_0)_{Pd(annealing+current\ flow)} = a_{3,1}\left(1 - exp\left(-\frac{t}{\tau_{3,1}}\right)\right) + a_{3,2}\left(1 - exp\left(-\frac{t}{\tau_{3,2}}\right)\right) + a_{3,3}\left(1 - exp\left(-\frac{t}{\tau_{3,3}}\right)\right) \quad (6.6)$$

6.3 Regression Analysis of the Hydrogen Release Mechanisms by Applying Current Flow during Annealing

Fig. 6.3 shows the change in current value of p-type GaN/Ni and p-type GaN/Pd contacts during annealing at 673 K with and without applying current flow under condition of 10 V. When the current was measured, the voltage was reduced from 10 V to 1.0 V. The results show that, the electrical conduction of all three contacts are improved by the annealing. In the case of annealing p-type GaN/Ni contact at 673 K without applying the current flow, the electrical conduction of the contact shows some improvement up to 660 s into the annealing. It is worthwhile to be mentioned that up to 660 s into the annealing, p-type GaN/Ni contact annealed without applying the current flow show greater improvement in electrical conduction compared to the p-type GaN/Ni

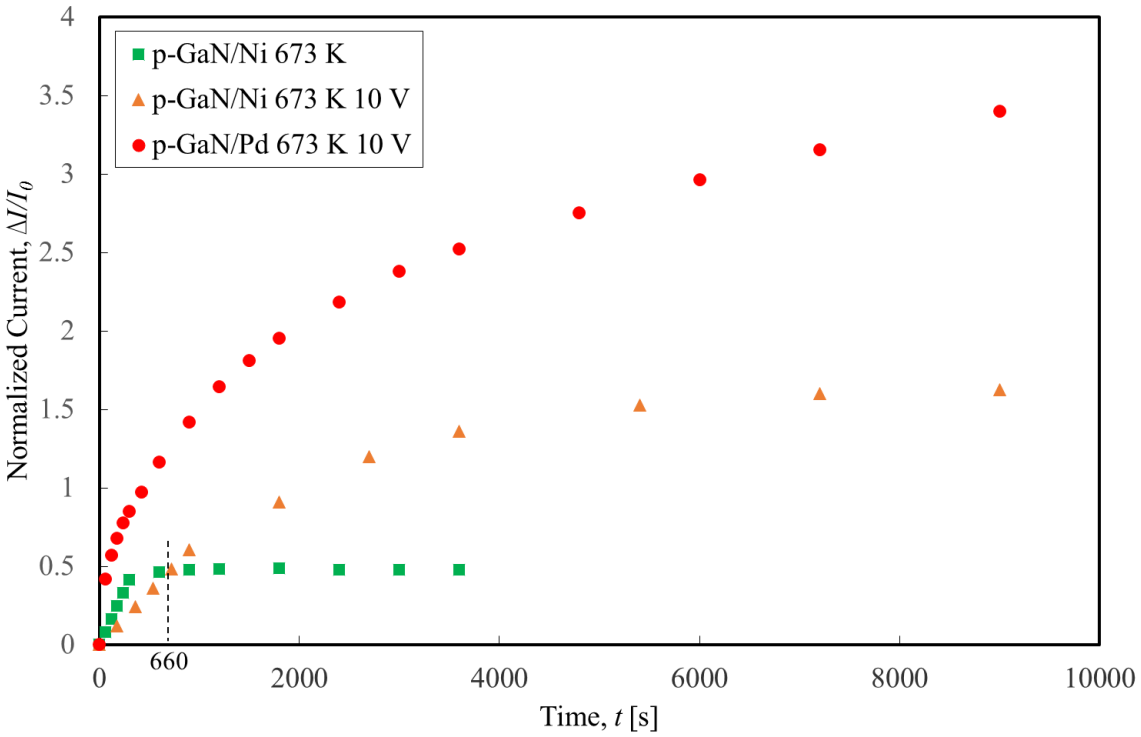

Fig. 6.3 Change in current value of contacts during annealing at 673 K; p-type GaN/Ni contact annealed without applying current flow, p-type GaN/Ni and p-type GaN/Pd contacts annealed while applying current flow under condition of 10 V. ($\Delta I = I - I_0$, I: current value for V = 1.0 V, I_0: current Value for V = 1.0 V at t = 0 s).

contact annealed with the current flow applied. However, after 660 s into the annealing, the current value of the contact annealed without applying the current flow starts to saturate. On the other hand, the electrical conduction of the contact annealed with the current flow applied keeps increasing until 8000 s into the annealing before starts to saturate.

These results indicate that indeed the mechanisms of H release from GaN are working dependently to each other. By applying current flow during annealing, the mechanism of H release through exposed p-type GaN surface by the thermal annealing is weaken, therefore less improvement of electrical conduction achieved at the early stage of the annealing. However, by prolonging the annealing, compared to without applying the current flow, greater amount of H can be released from GaN by applying the current flow.

In the case of p-type GaN/Pd contact annealed with the current flow applied, from the early state of annealing, this contact shows the greatest improvement in electrical conduction compared to other contacts. Furthermore, the current value of this contact is still increasing even after annealing for 10000 s. These results indicate the additional mechanics of H release introduced by using Pd contact has enhance the H release and further improved the electrical conduction of the p-type GaN contact. However, it is important to mentions that the I_0 (current value for V = 1.0 V, t = 0 s at 673 K) of the p-type GaN/Pd contact is much lower than I_0 of the p-type GaN/Ni contact, which are 0.12 mA and 0.22 mA, respectively. Due to the high work function value (5.1 eV), Ni is known to be an adequate contact material for p-type GaN. On the other hand, Pd has a slightly lower work function (5.0 eV) compared to Ni. Furthermore, it is known that by the presence of H within Pd, the work function is reduce and the Pd resistance is increase.

The unstable nature of Pd made it not considered as an adequate contact materials for p-type GaN. Despite the fact that Pd is not an adequate contact material for p-type GaN, p-type GaN/Pd contact show the greater improvement in electrical conduction compared to p-type GaN/Ni contact, as shown by the normalized current values in Fig. 6.3. These results suggest that by using Pd as contact materials instead of Ni, significantly greater amount of H can be released from GaN.

To analyze these results and understand the mechanisms of H release for these three models, regression analysis method was applied. By using kinetic model and least square method, regression curves that best fit the measured current values are drawn. The least square method is describe as following: (1) Several sets initial values of a and τ are considered for each k (H release mechanisms). (2) The set with minimum residual sum of square (minimum difference between the measured current values and the current value obtain by kinetic model) is determined. (3) Several new initial values are chosen iteratively based on the previous set with minimum residual sum of square. (4) The procedure is repeated to obtain successive approximations of a converged minimum of each a and τ values.

Fig. 6.4 show the regression analysis of the measured current value of p-type GaN/Ni contacts during annealing at 673 K with and without applying current flow under condition of 10 V. By using the kinetic model shown in Eq. (6.4) and (6.5), the regression curves corresponding to the change in current value of p-type GaN/Ni contact during annealing without and with the current flow applied can be expressed by the following equations, respectively.

$$(\Delta I/I_0)_{Ni(annealing)} = 0.5\left(1 - exp\left(-\frac{t}{230}\right)\right) \tag{6.7}$$

$$(\Delta I/I_0)_{Ni(annealing+current\ flow)} = 0.1\left(1 - exp\left(-\frac{t}{1000}\right)\right) + 1.55\left(1 - exp\left(-\frac{t}{2200}\right)\right) \quad (6.8)$$

As shown in these equations, the saturation value, $a_{1,1}$ and the exponential decay with time constant, $\tau_{1,1}$ for the first model are 0.5 and 230, respectively. For the second model, the saturation values, $a_{2,1}$ and $a_{2,2}$ are 0.1 and 1.55, and the exponential decay with time constant, $\tau_{2,1}$ *and* $\tau_{2,2}$ are 1000 and 2200, respectively. The curves marked as (1) in Fig. 6.4 is correspond to the amount of H released through exposed p-type GaN surface by the thermal annealing ($a_{2,1}$ and $\tau_{2,1}$) of the second model (Eq. 6.8). The curves marked as (2) in Fig. 6.4 is correspond to the amount of H released through the contact interface by applying current flow during annealing ($a_{2,2}$ and $\tau_{2,2}$)

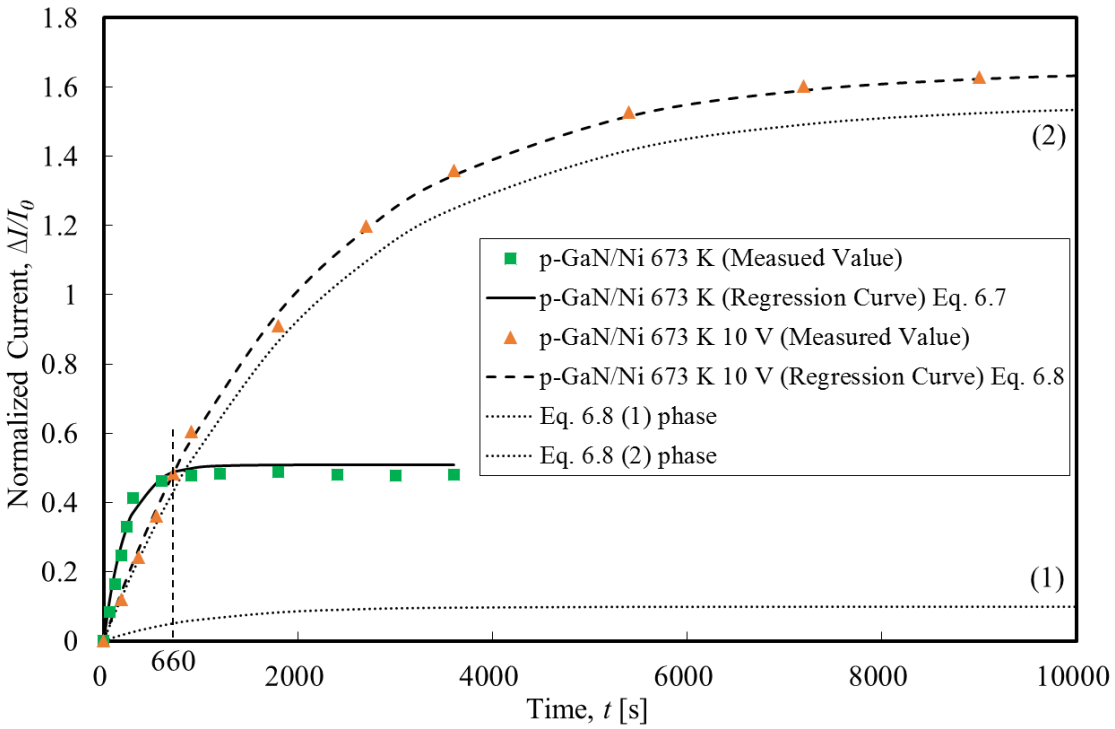

Fig. 6.4 Regression analysis of change in current value of p-type GaN/Ni contacts during annealing at 673 K with and without applying current flow under condition of 10 V. ($\Delta I = I - I_0$, I: current value for V = 1.0 V, I_0: current Value for V = 1.0 V at t = 0 s).

As discussed in the kinetic model of the second model, H is moved near the interface between p-type GaN and Ni contact by the applied current flow. This H movement reduce the H concentration of other area of p-type GaN, and subsequently reduce the amount of H released through exposed p-type GaN surface by thermal annealing. These interaction between the mechanisms of H release can be observed by comparing the saturation values, a and the exponential decay with time constant, τ of each model. The smaller value of $a_{2,1}$ (0.1) compared to $a_{1,1}$ (0.5) indicate that the amount of H released in the first mechanism of second model compared to first model have decrease. Furthermore, the higher $\tau_{2,1}$ value (1000) in second model compared to the $\tau_{1,1}$ (230) indicate that the rate of H released by this mechanism has become slower. Hence, at the early stage of the annealing, greater improvement of electrical conduction is achieved by annealing the p-type GaN/Ni contact at 673 K without applying the current flow.

For the second mechanism of H release, the values of $a_{2,2}$ and $\tau_{2,2}$ are much higher compared to the first mechanism. The higher value of a indicate that significantly greater amount of H is released by the mechanism in the second mechanism (H diffuse along the contact interface), i.e., greater improvement of electrical conduction of p-type GaN/Ni contact is achieved by applying current flow during annealing. Furthermore, the higher value of τ indicate that this mechanism of H release is occurring much slower and longer before start to saturate, i.e., longer annealing time is needed before the significant improvement of electrical conduction can be achieved.

Fig. 6.5 show the regression analysis of the measured current value of p-type GaN/Pd contact during annealing at 673 K while applying the current flow under condition of 10 V. By using the kinetic model shown in Eq. (6.6), the regression curve corresponding to the change in current value of p-type GaN/Pd contact during annealing

while applying the current flow can be expressed by the following equation.

$$(\Delta I/I_0)_{Pd(annealing+current\ flow)} = 0.4\left(1 - exp\left(-\frac{t}{50}\right)\right) + 1.0\left(1 - exp\left(-\frac{t}{800}\right)\right) + 2.8\left(1 - exp\left(-\frac{t}{7000}\right)\right) \quad (6.9)$$

As shown in this equations, the saturation values for each mechanisms in this third model, $a_{3,1}$, $a_{3,2}$ and $a_{3,3}$ are 0.4, 1.0 and 2.8, respectively. The exponential decay with time constant for each mechanisms in this model, $\tau_{3,1}$, $\tau_{3,2}$ and $\tau_{3,3}$ are 50, 800 and 7000, respectively. The curves marked as (1), (2) and (3) in Fig. 6.5 are correspond to the first mechanism ($a_{3,1}$ and $\tau_{3,1}$), the second mechanism ($a_{3,2}$ and $\tau_{3,2}$) and the third mechanism ($a_{3,3}$ and $\tau_{3,3}$) of H release in this model, respectively. The curves marked as (1), (2) and (3) in Fig. 6.5 are correspond to the first mechanism ($a_{3,1}$ and $\tau_{3,1}$), the second

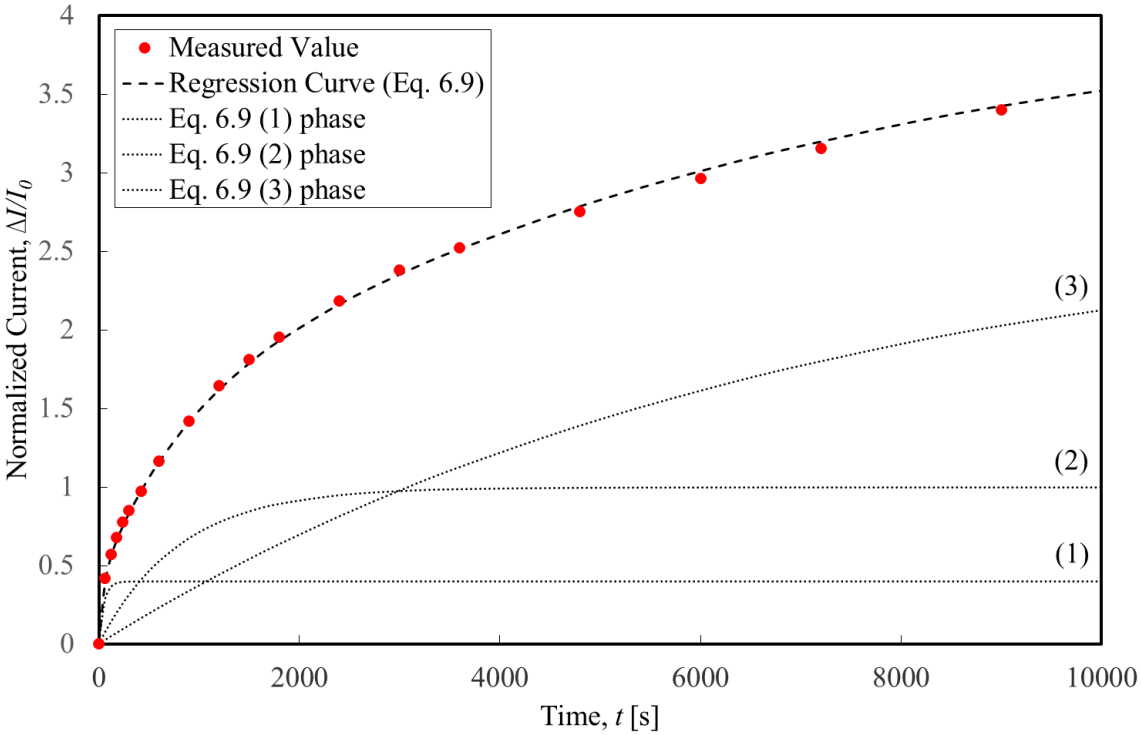

Fig. 6.5 Regression analysis of change in current value of p-type GaN/Pd contact during annealing at 673 K while applying current flow under condition of 10 V. ($\Delta I = I - I_0$, I: current value for V = 1.0 V, I_0: current Value for V = 1.0 V at t = 0 s).

mechanism ($a_{3,2}$ and $\tau_{3,2}$) and the third mechanism ($a_{3,3}$ and $\tau_{3,3}$) of H release in the third model (Eq. 6.9), respectively.

The saturation value $a_{3,3}$ (2.8) and the exponential decay with time constant $\tau_{3,3}$ (7000) of the third mechanism of H release (H release through Pd film by applying current flow during annealing) are highest compared to the saturation values and exponential decay with time constant of other mechanisms of all the models. These values indicate that the H release has been significantly enhanced by this mechanism. Greater amount of H is released and the mechanism of H release occurring much longer before start to saturate. As shown in the Fig. 6.5, the current value is still increasing even after annealing for 10000 s, i.e., the H release is still occurring and electrical conduction of the contact is keep improved even after annealing for 10000 s.

From these results, it can be understand that by applying current flow during annealing and forming a contact with material that H can diffuse into, the H release from GaN substrate can be enhanced and the electrical conduction of p-type GaN contact can be significantly improved.

6.4 Summary

In this chapter, in order to improve the electrical conduction of Mg-doped p-type GaN contacts, enhancement of hydrogen release from GaN substrates is attempted. The electrical conduction profiles of the p-type GaN/Ni contact annealed at 573 K and 673 K for 3600 s while subjected to current flow show some improvement compared to the contact annealed without applying the current flow. From these results, it can be understood that by applying current flow through the GaN substrates during annealing process, hydrogen release form GaN substrates can be enhanced by even annealing at low

temperature. To understand the mechanism of hydrogen release by applying current flow during annealing, the change in current values p-type GaN contacts during annealing has been observed. By using regression analysis and kinetic model, the electrical conduction improvement achieve by applying current flow through GaN substrate during annealing have been analysis. The results suggest that that by applying current flow during annealing and by forming a contact with material that H can diffuse into such as Pd, the H release from GaN substrate can be enhanced and the electrical conduction of p-type GaN contact can be significantly improved.

References:

[1] S. J. Pearton, J. C. Zolper, R. J. Shul, and F. Ren, "GaN: Processing, defects, and devices," Journal of Applied Physics 86, No. 1 (1999), 1-78.

[2] S. Nakamura, N. Iwasa, M. Senoh, and T. Mukai, "Hole Compensation Mechanism of P-Type GaN Films," Japanese Journal of Applied Physics 31 (1992), 1258-1266.

[3] J. Neugebauer and C. G. Van De Walle, "Hydrogen in GaN: Novel Aspects of a Common Impurity," Physics Review Letters 75, No. 24 (1995), 4452-4455.

[4] B. Clerjaud, D. Cote, A. Lebkiri, C. Naud, J. M. Baranowski, K. Pakula, D. Wasik, and T. Suski, "Infrared spectroscopy of Mg-H local vibrational mode in GaN with polarized light," Physical Review B 61, No. 12 (2000), 8238-8241.

[5] S. M. Myers, C. H. Seager, A. F. Wright, B. L. Vaandrager, and J. S. Nelson, "Electron-beam dissociation of the MgH complex in p-type GaN," Journal of Applied Physics 92, No. 11 (2002), 6630-6635.

[6] S. Nakamura, T. Mukai, M. Senoh and N. Iwasa, “Thermal Annealing Effects on P-Type Mg-Doped GaN Films,” Japanese Journal of Applied Physics 31 (1992), L139- L142.

[7] A. b. M. Halil, K. Tsuchida, M. Maeda and Y. Takahashi, “Ni Nano Level Thin Film Formation on p-GaN and Improvement of Electrical Properties by Hydrogen Release Enhancement,” Journal of Smart Processing 4, No. 2 (2015) 109-114.

[8] S. M. Myers, A. F. Wright, G. A. Petersen, C. H. Seager, W. R. Wampler, M. H. Crawford, and J. Han, “Equilibrium state of hydrogen in gallium nitride: Theory and experiment,” Journal of Applied Physics 88 (2000), 4676-4687.

[9] L. L. Jewell and B. H. Davis, “Review of absorption and adsorption in the hydrogen–palladium system,” Applied Catalysis A: General 310 (2006), 1-15.

[10] S. Hara, A. Caravella, M. Ishitsuka, H. Suda, M. Mukaida, K. Haraya, E. Shimano and T. Tsuji, “Hydrogen diffusion coefficient and mobility in palladium as a function of equilibrium pressure evaluated by permeation measurement,” Journal of Membrane Science 421-422 (2012), 355-360.

Chapter 7: Conclusions

To improve the electrical conduction of n-type GaN contact, formation of sufficient N-vacancies within GaN sub-surface, adequate surface orientation of GaN and subsequent annealing condition has to be determined by considering the reaction occur between deposited film and GaN substrate.

Ti contact films were formed on n-type GaN after Ar ion irradiation of the substrate for 300, 600, 1200, 2400 and 3600 s. Ti_2N is formed adjacent to substrate by the Ti deposition. It is likely that a huge amount of N-vacancies is formed within the GaN sub-surface near to the contact. *I-V* conduction profiles show that ohmic conduction is achieved. Furthermore, the conductance of the contacts is increased by prolonging the irradiation time. However, extensive irradiation more than 3600 s shows no further improvement in contact conductance. It is likely due to the phase transformation from GaN to Ga-rich at the GaN sub-surface. The Ga-rich phase enhanced the formation of Ti-Ga compound at the interface during the Ti deposition and reduce the number of N-vacancies within the sub-surface of GaN.

Ti contact films were formed on various orientation of GaN surface. The contact formed on (0001) Ga-face shows the highest electrical conduction in the as-deposited state. However, the conduction deteriorates by annealing even at a low temperature of 773 K. On the other hand, the conductance of the contacts on other three surfaces shows some improvement by annealing at 973 K. However the conductance deteriorates by further annealing at 973 K for 300s. The deterioration of the electrical conductance is attributed to the formation of Ti-Ga compound at the interface, as shown in the XRD patterns and TEM observation.

To the investigation of the interfacial structure of GaN and Ti_3SiC_2, Ti-Si-C ternary film with a composition stoichiometrically close to Ti_3SiC_2 has been deposited on p-type GaN. Polycrystalline Ti_3SiC_2 phase has been formed on the substrate after annealing at 973 K and 1073 K. However, after the annealing at 973 K and 1073 K, the dominant carrier-type of p-type GaN has inverted to n-type. This is likely due to the increasing of N-vacancies in the p-type GaN sub-surface resulting from the out-diffusion of N atoms during the annealing at high temperature. The direct-current conduction test shows that ohmic-like contacts have been achieved after the annealing. These ohmic-like contacts are likely formed between n-type GaN (inverted from p-type by the annealing) and the byproducts of Ti_3SiC_2 formation (Ti_5Si_3 and $TiSi_2$), the residual Ti phase and/or the TiN phase.

The investigation of the interfacial structure and electrical conduction of p-type GaN/Au and p-type GaN/Ni contacts after annealing at 673 K for 3600 s show some identical results. The dominant carrier-type of both contacts are maintained after the annealing. XRD analysis and TEM observation of both contacts revealed that the no intermetallic compound is formed at the interface after the annealing. Furthermore, the electrical conduction profile of these contacts show some improvement after the annealing at 573 K and 673 K for 3600 s. From these investigations, it can be conclude that annealing at 673 K for 3600 s is an adequate annealing condition to form Au and Ni contact on p-type GaN, while improving the electrical conduction and while maintaining the p-type carrier.

In order to improve the electrical conduction of Mg-doped p-type GaN contacts, enhancement of hydrogen release from GaN substrates is attempted. The electrical conduction profiles of the p-type GaN/Ni contact annealed at 573 K and 673 K for 3600

s while subjected to current flow show some improvement compared to the contact annealed without applying the current flow. From these results, it can be understood that by applying current flow through the GaN substrates during annealing process, hydrogen release form GaN substrates can be enhanced by even annealing at low temperature. To understand the mechanism of hydrogen release by applying current flow during annealing, the change in current values p-type GaN contacts during annealing has been observed. By using regression analysis and kinetic model, the electrical conduction improvement achieve by applying current flow through GaN substrate during annealing have been analysis. The results suggest that that by applying current flow during annealing and by forming a contact with material that H can diffuse into such as Pd, the H release from GaN substrate can be enhanced and the electrical conduction of p-type GaN contact can be significantly improved.

Acknowledgement:

Firstly, I would like to express my sincere gratitude to my supervisor Prof. Takahashi Yasuo for the continuous support of my Ph.D study and related research, for his patience, motivation, and immense knowledge. His guidance helped me in all the time of research and writing of this thesis. I could not have imagined having a better supervisor and mentor for my Ph.D study.

Besides my supervisor, I would like to thank the rest of my thesis reviewers: Prof. Itou Kazuhiro and Prof. Hirata Yoshinori, for their insightful comments and encouragement, but also for the hard question which incented me to widen my research from various perspectives.

I thank my fellow lab mates in for the stimulating discussions, for the sleepless nights we were working together before deadlines, and for all the fun we have had in the last three years. In particular, I am grateful to Mr Maeda Masakatsu for enlightening me the first glance of research.

I would like express their gratitude to Prof. H. Mori and Mr. E. Taguchi for their kind permission and assistance to use facilities in the Research Center for Ultra-High Voltage Electron Microscopy, Osaka University, Japan.

Last but not the least, I would like to thank my family: my wife, my parents, my sisters and to my in-law-family for supporting me spiritually throughout writing this thesis and my life in general.

Achievement:

Chapter 4

[1] A. b. M. Halil, K. Kimura, M. Maeda and Y. Takahashi, "Microstructures Observation of N-type GaN Contacts and the Electrical Properties," Transactions of JWRI 44, No. 1 (2015), 19-22.

[2] K. Kimura, A. b. M. Halil, M. Maeda and Y. Takahashi, "Effect of crystal orientation on ohmic contact formation for n-type gallium nitride," IOP Conference Series: Materials Science and Engineering 61 (2014), 012033.

Chapter 5

[3] A. b. M. Halil, M. Maeda and Y. Takahashi, "Electrical properties and structure of contact interface between Ti_3SiC_2 and p-type GaN," Journal of Physics: Conference Series 379 (2012), 012021.

[4] A. b. M. Halil, M. Maeda and Y. Takahashi, "Interfacial Nanostructure and Electrical Properties of Ti_3SiC_2 Contact on p-Type Gallium Nitride," Materials Transactions 54, No. 6 (2013) 890-894.

[5] A. b. M. Halil, M. Maeda and Y. Takahashi, "Effect of Ti_3SiC_2 formation on p-type GaN by vacuum annealing on the contact properties," IOP Conference Series: Materials Science and Engineering 61 (2014) 012034.

Chapter 6

[6] A. b. M. Halil, K. Tsuchida, M. Maeda and Y. Takahashi, "Improvement of Electrical Properties of p-type GaN and Au Contact Interface," Quarterly Journal

of the Japan Welding Society 33, No. 2 (2015) 84s-87s.

[7] A. b. M. Halil, K. Tsuchida, M. Maeda and Y. Takahashi, “Ni Nano Level Thin Film Formation on p-GaN and Improvement of Electrical Properties by Hydrogen Release Enhancement,” Journal of Smart Processing 4, No. 2 (2015) 109-114.